

# Insights into Optoelectronic Polymer- Neuronal Interface

*A Thesis*

*submitted in partial fulfillment for the degree of*

**MASTER OF SCIENCE**

*as a part of the Integrated Ph.D. programme*

**(Materials Science)**

by

**VIKAS GARG**



CHEMISTRY AND PHYSICS OF MATERIALS UNIT  
JAWAHARLAL NEHRU CENTRE FOR ADVANCED SCIENTIFIC  
RESEARCH  
(A Deemed University)  
Bengaluru, INDIA  
April 2015

**To my Parents...**



## DECLARATION

I hereby declare that this thesis entitled “**Insights into Optoelectronic Polymer-Neuronal Interface**” is an authentic record of the research work carried out by me under the supervision of Prof. K. S. Narayan at the Chemistry and Physics of Materials Unit, Jawaharlal Nehru Centre for Advanced Scientific Research, Bengaluru, India, and it has not been submitted anywhere for the award of any degree or diploma.

In keeping with the general practice of reporting scientific observations, due acknowledgements has been made whenever work described here has been based on the findings of other investigators. Any omission that might have occurred due to oversight or inadvertence in judgment is deeply regretted.

Date:

Place: Bengaluru, India

Vikas Garg



## Jawaharlal Nehru Centre for Advanced Scientific Research

Jakkur, Bangalore 560064, India

K. S. NARAYAN  
Professor and Dean (R&D)  
PHONE: 91 80 22082822  
FAX: 91 80 22082766  
e-mail: narayan@jncastr.ac.in

URL: [www.jncastr.ac.in/narayan](http://www.jncastr.ac.in/narayan)



---

April 15, 2015

### Certificate

I hereby certify that the matter embodied in this thesis entitled “**Insights into Optoelectronic Polymer-Neuronal Interface**” has been carried out by Mr. Vikas Garg at the Chemistry and Physics of Materials Unit, Jawaharlal Nehru Centre for Advanced Scientific Research, Bangalore, India under my supervision and that it has not been submitted elsewhere for the award of any degree or diploma.

Prof. K.S. Narayan  
(Research Supervisor)



## Acknowledgements

I express my deep felt gratitude for my research supervisor Prof. K.S. Narayan for his constant guidance, unstinted support, and timely suggestions throughout my M.S. research tenure. I am grateful to him for supporting me in propelling my research project in the right direction. I am indebted to him for the acquired skills in several instrumental techniques during my research practice.

I am grateful to Prof. C.N.R Rao for being a constant source of inspiration during my stay in the JNCASR campus. His presence and warmth itself is a motivation for performing scientific research.

I am grateful to Prof. Uday Kumar Ranga, Molecular Biology and Genetics Unit, JNCASR for allowing me to work and learn in his lab. I sincerely acknowledge him for providing the lab facilities as well as guidance whenever needed.

I am specially thankful to Malini who helped me in the hour of need when hopes were low. She taught me, how to handle small lives in a petri dish. Without her help and constant motivation, this thesis would have not be possible.

I am deeply grateful to our chairman, Prof. S. Balasubramanian and Integrated Ph.D. coordinator, Prof. T.K. Maji for their support at times of distress and extending their help to overcome all the challenges of research endeavor. I express my sincere thanks to all the teachers from CPMU, NCU, MBGU, TSU and NCBS for teaching me and helping me in clearing my fundamentals.



I would like to thank all the teachers who taught me till now. They are the people who instilled the knowledge in me. Especially, I am very much grateful to Prof. P.N. Pandit whose discipline in practice of physics stimulated an indomitable interest in me. His constant support and encouragement helped a little boy in finding his way to life.

I am thankful to all my present and past labmates Ravi, Prashant, Ashar, Swathi, Raaghesh, Rishav, Apoorva, Manjunath, Nisha, Krishna, Anshuman, Vini, Satya, Dhruv and Jefin for stimulating work environment in the lab. I am deeply grateful to Dr. DHK Murthy for motivation and support during my stay in lab. He was the one who taught me how to persevere your dreams even if times are not good. I am also thankful to all the members of HIV-AIDS lab for useful discussions and cooperation while working there.

I am deeply thankful to my batch mates, Shantanu, Shivakumar, Sohini, Rajkumar and Promit for making the classes and laboratory fun without compromising the learning part. I am especially thankful to Shivakumar for making the environment competitive enough to accelerate the learning process.

I am really indebted to my friends in JNCASR, Sunil, Dheeraj, Sanjay, Devinder, Rajdeep, Chandan, Ankush, Guratinder, Sukanya and Chaitra for making it a wonderful time in JNCASR. They were always there with me, be it a time of frustration or celebrations.

I am also indebted to my friends outside JNCASR, Priya, Luxmi, Pravesh, Karun, Monica and Anurag. They really proved that distances do not matter when bonds are truly strong.

I thank all the staff members of JNCASR for their assistance throughout my stay in JNCASR. Especially, Dr. Prakash from Animal Facility, Mr. Alla Srinivas Rao from Integrated Ph.D. Physics Laboratory, Mr. Lakkappa and Mr. Sridhar from HIV-AIDS lab for making my life easy. They are the people who really made things moving.

Lastly, I can't express my deep gratitude for my respected parents, caring brother and family in words.

Vikas Garg



# Abbreviations

AMD.....	Age-related Macular Degeneration
ANOVA.....	Analysis of Variance
BHJ.....	Bulk Hetero-Junction
CCD.....	Charge Coupled Device
DIV.....	Days <i>in vitro</i>
DMEM.....	Dulbecco Modified Essential Medium
EBSS.....	Earle's Balanced Salt Solution
EDTA.....	Ethylene Diamine Tetraacetic Acid
El.....	Electrolyte
HOMO.....	Highest Occupied Molecular Orbital
IPCE.....	Incident Photo to Charge Carrier Efficiencies
ITO.....	Indium Tin Oxide
LUMO.....	Lowest Unoccupied Molecular Orbital
MEA.....	Multi Electrode Arrays
N2200.....	poly{[N,N'-bis(2-octyldodecyl)-naphthalene-1,4,5,8-bis(dicarboximide)-2,6-diy]-alt-5,5'-(2,2'-bithiophene)}
NIR.....	Near- Infra Red
OFET.....	Organic Field Effect Transistor
P3HT.....	Poly-(3-hexylthiophene)
PBS.....	Phosphate Buffered Saline
PEDOT:PSS.....	Poly(3,4-ethylenedioxythiophene) polystyrene sulfonate
RP.....	Retinitis Pigmentosa
SEM.....	Standard error in Mean

# Outline

Retinitis pigmentosa (RP) and Age-related Macular Degeneration (AMD) are two malfunctioning states of the visual system in which the photoreceptor layer of the retina is partially or completely non-functional resulting in partial or complete blindness, although rest of the optical and neuronal machinery of the visual system is fully functional. Artificial retinal implant which is an array of microelectrodes, is one the latest approach to circumvent this issue. This array of electrodes is connected to an imaging device that converts the incoming light signals into electrical signals. The microelectrode array excites the neurons of the retina in close proximity using these electrical signals and evokes the perception of vision.

Optoelectronic polymers is one important class of materials having unique combination of electronic and optoelectronic properties coupled with improved biocompatibility which has the potential for future neuroprosthetic devices. Freedom to tune their absorption range opens up the possibilities for augmented vision in humans with sensitivity for an extended range of electromagnetic spectrum. Optoelectronic polymers generate electric potentials in response to light. They are mechanically soft and conformable. They can also be used for simultaneous optical stimulation and electrophysiological recordings. Neuronal cell differentiation and controlled drug delivery are other important applications of these materials.

Optoelectronic semiconducting polymers form an integral part of the work described in this thesis. This thesis deals with the long term effects of biological

environment on functionality and stability of these optoelectronic polymers when present as a functional device. This thesis also addresses the inverse question, which is, effects on biological systems when in contact with optoelectronic polymers for a prolonged duration.

Chapter 1 introduces the optoelectronic polymers and the basic mechanisms governing the unique properties in them. Mechanism of neuronal action and anatomy of the retina is also discussed very briefly.

Chapter 2 deals with the studies on stability and functionality of optoelectronic polymer based devices when exposed to physiological conditions for a long time. This has implications in assessment of optoelectronic devices for neuroprosthetic implants.

Chapter 3 describes the effects of optoelectronic polymers on biological systems in terms of cytotoxicity and biocompatibility over a long duration of time.

Chapter 4 tells about the future directions in the field of development of neuroprosthetic implants using optoelectronic polymers as well as about the possibilities of novel optical stimulation techniques in electrophysiology using optoelectronic polymers.

# Contents

<b>Chapter 1: Introduction.....</b>	<b>1</b>
1.1 Motivation.....	1
1.2 Conjugated Semiconducting Polymers.....	4
1.2.1 Properties of Conjugated Polymers.....	5
1.2.2 Optoelectronic Polymers.....	6
1.3 Electrical Processes in Neurons.....	9
1.3.1 Action Potential.....	10
1.3.2 Recording Techniques.....	12
1.4 Retina.....	13
<b>Chapter 2 : Long term stability of polymer/electrolyte interfaces under physiological conditions.....</b>	<b>15</b>
2.1 Introduction.....	15
2.1.1 Semiconductor/Electrolyte Interfaces.....	16
2.1.2.... Polymer/Electrolyte Interfaces.....	17
2.1.3 Polymer Based Biointerfaces.....	18
2.2 Experimental Section.....	19
2.2.1. Experimental Strategy.....	19
2.2.2 Materials Used.....	20
2.2.3 Device Fabrication.....	20
2.2.4 Photoillumination and Photovoltage Measurement Setup.....	22
2.3 Results.....	24
2.4 Discussions.....	28

**Chapter 3 : Optoelectronic semiconducting Polymers as Active Biocompatible Interfaces for Neuronal cells.....31**

3.1.... Introduction..... 31

3.2 Experimental Section..... 32

    3.2.1.Materials Used..... 32

    3.2.2. Fabrication of Polymer Thin Films..... 32

    3.2.3 Sterilization of Polymer Films for Cell Culture..... 33

    3.2.4 Ornithine/Laminin Treatment ..... 33

    3.2.5. Preparation of Immortal Cell Lines ..... 34

    3.2.6 Extraction of Primary Retinal Cells ..... 35

    3.2.7. Photoillumination Setup..... 36

3.3 Observations & Analysis..... 36

3.4 Results & Discussions..... 37

**Chapter 4 : Summary & Future Directions.....43**

**References.....45**

**Appendix**

    Arduino Code for Photoillumination Setup ..... i

    LabVIEW Program for Interfacing Arduino and Oscilloscope ..... ii



# List of Figures

Figure 1.1 : Chemical structures of some common conjugated polymers.....	5
Figure 1.2 : Energy level diagram for a bulk hetero junction system, photo-excitation and charge diffusion toward electrodes.....	7
Figure 1.3 : Charge separation at a donor/acceptor interface in a bulk heterojunction interface.....	8
Figure 1.4 : Structure of a typical neuron.....	9
Figure 1.5 : Schematic showing course of action potential with time.....	11
Figure 1.6 : Structure of human eye with inverted retina at the back and multilayered structure of retina.....	14
Figure 2.1: Schematic showing the space charge layers when n-type semiconductor is brought in contact with an electrolyte. (a) Distribution of charge carriers (b) Course of band edges (c) Course of electric potential. Redrawn from [36].....	16
Figure 2.2 : Chemical structures of (a) P3HT, (b) N2200, (c) relative energy levels of P3HT and N2200 (d) and normalized absorption spectrum of BHJ consisting of P3HT and N2200.....	21
Figure 2.3 : Schematic showing the experimental setup (Not to scale).....	23
Figure 2.4 : Image displaying polymer/electrolyte devices with Arduino.....	23
Figure 2.5: (a) Photovoltage profile for BHJ/electrolyte device when illuminated with LEDs of different color, (b) Emission spectra for different LEDs.....	25
Figure 2.6 : Long term normalized ( $V_{\text{peak}}/V_{\text{peak at } t=0}$ ) response of maxima and minima for (a) $\lambda = 644$ nm and (b) $\lambda = 520$ nm.....	26
Figure 2.7 : Long term normalized ( $V_{\text{peak}}/V_{\text{peak at } t=0}$ ) response of maxima and minima for ( $\lambda = 453$ nm).....	27
Figure 2.8 : Comparison between blue and curve obtained from summation of red and green.....	28
Figure 3.1 : Patterning the polymer strips on cover slip. Polymer is shown in blue..	31
Figure 3.2 : Eenucleated eye from a mice pup.....	34

Figure 3.3 : Photoillumination assembly for studying the effects of light. 3D printed culture plate holder is shown in yellow.....	35
Figure 3.4 : (a) Microscopic image of growth of SH-SH5Y cells on P3HT substrate, DIV 2, (b) Same image after edge detection. Difference in cell density is clearly evident in this image.....	36
Figure 3.5: (a) Microscopic image of growth of SH-SH5Y cells on N2200 substrate, DIV 2, (b) Same image after edge detection.....	37
Figure 3.6: (a) Microscopic image of growth of SH-SH5Y cells on polymer blend (P3HT: N2200) substrate, DIV 2, (b) Same image after edge detection.....	37
Figure 3.7: (a) Microscopic image of growth of SH-SH5Y cells on glass substrate for control experiments, DIV 2, (b) Same image after edge detection.....	37
Figure 3.8 : Histogram showing cell density comparison for P3HT and glass regions coexisting in the same well. Data are shown in mean + standard error in mean (SEM) configuration for the six images from the same well.....	38
Figure 3.9 : Histogram showing cell density comparison for N2200 and glass regions coexisting in the same culture well. Data are shown in mean + standard error in mean (SEM) configuration for the six images from the same culture well.....	38
Figure 3.10: Histogram showing cell density comparison for Blend system and glass regions coexisting in the same culture well. Data are shown in mean + standard error in mean (SEM) configuration for the six images from the same culture well.....	39
Figure 3.11 : Histogram showing comparison among cell densities in P3HT, N2200, Blend, N2200 and glass (control) experiments. Data are shown in mean + standard error in mean (SEM) configuration.*Significance against glass at $p < 0.05$ , **Significance against glass at $p < 0.02$ . (ANOVA test).....	39

# CHAPTER 1

## Introduction

### 1.1 Motivation

Vision is one the most important senses of the human body. In the evolution as well, visual system developed at a very early stage indicating the importance of this sensory mechanism. Retinitis pigmentosa (RP) and age-related macular degeneration (AMD) are two of the many malfunctioning states of the visual system in which the photoreceptor or the other neuronal layers of retina are partially or completely non-functional. This results in conditions like night, color or even complete blindness. Artificial retinal implant is one of the latest approach in curing the RP and AMD in which an array of electrodes is surgically implanted close to the retina. This array of electrodes is connected to an imaging device like a charged coupled device (CCD) that converts the external light signals into electrical signals. The microelectrode array receives these electrical signals from CCD and excites the neurons of the retina close proximity and elicit the perception of vision in the brain [1-3].

Novel materials with combinations of properties are sought for such kind of active and unique neuroelectronic implants (microelectrode array). Conjugated polymers with a unique combination of electronic properties and extraordinary biocompatibility are one of the promising material candidates in this niche. Organic semiconductors which is a subset of conjugated polymers, exhibit interesting

## Chapter 1

optoelectronic properties in addition, which have got a large number of advantages over the existing counter parts. For example, they generate charges and electric potentials in response to the light very efficiently. This makes them capable of generating power from the same light signal which was meant for seeing. Hence, they have the potential to work as an autonomous device without the use of any external power source [4]. Also, since the array itself is sensitive to light just as retina, any other imaging device to convert the light signals to electrical signals is not required. This also provides a unique soft interface with the cells that can be used to stimulate the retinal cells. Their absorption range varies from visible to near infrared and can be tuned to any desired level. This opens up the possibilities for augmented vision in humans with sensitivity for an extended range of electromagnetic spectrum.

Their inherent organic nature gives them an upper hand in terms of biocompatibility when compared to any other inorganic semiconductor counterparts [5]. They are flexible and mechanically conformable which makes it possible to implant them at any curved surface. It is also shown that they promote the growth of neurites when placed in close contact which means that they may have the ability to initiate the natural repair mechanism of the body. They can be loaded with drugs or other important molecules which can be released in a controlled fashion externally which got implications in controlled drug delivery, again meant for repair. They can be used in aqueous environments as well as for sensing and probing unlike other electronic components. It is the combination of all these unique properties in optoelectronic polymers which attracted the attention of scientific community in the

recent past. Their applications not only include optically active neuroprosthetics but they also have potential to be used in the development of soft electrodes with simultaneous optical stimulation (completely bypassing the genetic procedures usually followed in optogenetics) and recording electrophysiological signals.

Synthetic polymers have been extensively used for biomedical applications including biosensing, bio-diagnostics and therapy [6-9]. Their electronic properties are exploited in coupling them with electrically active tissues such as brain, heart and skeletal muscles [10, 11]. Optoelectronic properties are being utilized in stimulating the blind retinal explants optically [4, 12]. Nonetheless, the potential utility of optoelectronic properties of conjugated polymers is still underexplored comparative to the electronic properties. Integration of biological systems at cellular and systems level with these materials with inherent optoelectronic properties is still in the budding stage. However, considering the magnitude of efforts and resources invested by the community in this direction in the recent past, it has become extremely urgent to assess the stability and functionality of these materials over a long period of time in the physiological conditions.

Optoelectronic semiconducting polymers form an integral part of the work described in this thesis. This thesis deals with the long term effects of biological conditions on functionality and stability of these optoelectronic polymers when present in functional device geometry and also the reverse, that is, the effects on biological systems when exposed to optoelectronic polymers for a long time. The answers to these questions lie in an interdisciplinary area of research and need an understanding of materials properties, biological phenomena and their interfaces.

## Chapter 1

In the following sections of this chapter, some of the relevant aspects of polymers as well as neuroscience are briefly discussed.

### 1.2 Conjugated Semiconducting Polymers

Conjugated polymers are unsaturated organic molecules having alternate single and double bonds along the carbon backbone chain. They conduct electricity (conductivity > 1500 S/cm) due to presence of delocalized  $\pi$ -electron system in the conjugated polymeric backbone. In the conjugated systems, hybridized  $sp^2$  orbitals are present on each carbon atom unlike saturated carbon counterparts where all carbons are present in  $sp^3$  hybridized state. The remaining unhybridized  $p_z$  orbital, orthogonal to the three sigma bonds ( $sp^2$ ) is present on each carbon atom. These  $p_z$  orbitals overlap to form one dimensional electronic band. Electrons in this band have high mobility comparative to other sigma bonded electrons.

According to the molecular orbital theory, one bonding and one antibonding molecular orbital are formed whenever two atomic orbitals overlap to form a bond. In ground state, electrons occupy the bonding molecular orbital prior to antibonding orbitals because of their low energy. The highest occupied molecular orbital (HOMO) and the lowest unoccupied molecular orbital (LUMO) are analogous to the valence and conduction bands in inorganic semiconductors. The difference of the HOMO and LUMO dictates the band gap in conjugated polymers. Conjugated polymers can behave as good conductors as well as semiconductors[13] depending upon the band gap. Chemical structures of few of commonly used conjugated polymers are shown in the Figure 1.1.

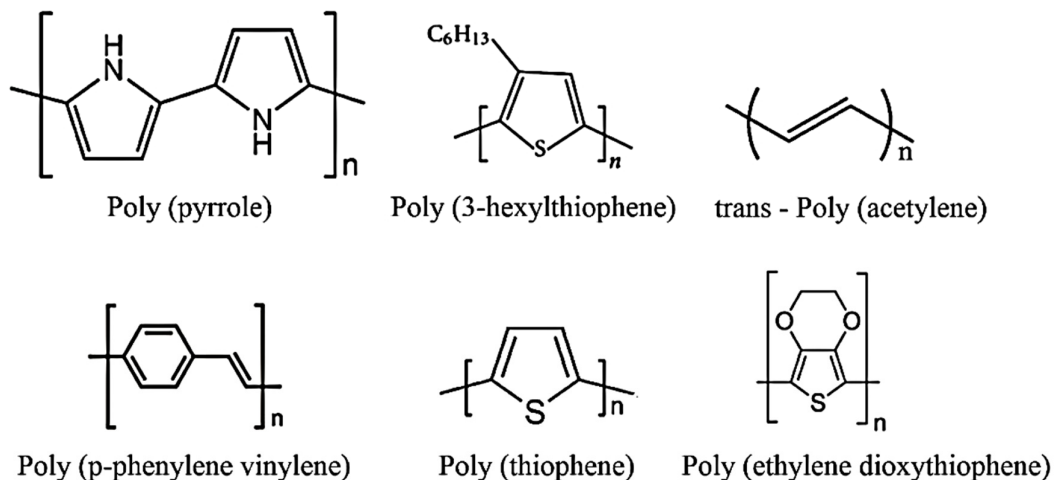


**Figure 1.2 : Chemical structures of some common conjugated polymers.**

By tailoring the number and type of substituents, length of the conjugated  $\pi$ -electron system as well as dopants; electronic properties like band gap and molecular orbital energy levels can be tuned to desired values. They exhibit both electronic as well as ionic conductivities in doped state. Doping is usually achieved through chemical or electrochemical means [13] which results in partial removal or addition of electrons/ions from the polymer backbone.

These polymers can be processed using solution based methods like drop casting, spin coating and dip coating, and can be printed on flexible and conformal substrates. As a consequence, organic semiconducting polymers are extensively used in the fields like flexible solar cells and curvilinear flexible electronics [14-17].

### 1.2.1 Properties of Conjugated Polymers

In conjugated polymers, charge carriers are mainly interpreted as quasi-particles namely polarons, solitons or bipolarons. These particles are formed because of structural deformation over several repeating units of polymer chains. In

## Chapter 1

optoelectronic polymer incidence of light is another useful way to generate charge carriers which is discussed in detail in the next section.

Unlike inorganic semiconductors, there exists localized states in organic semiconductors because of discontinuity in the conjugation of the polymeric backbone. As a consequence, conjugated polymers exhibit phonon assisted hopping mechanisms for charge transport. Typical values of mobility for organic semiconductors is  $\sim 0.01 \text{ cm}^2\text{V}^{-1}\text{s}^{-2}$  in comparison to  $\sim 1 - 1000 \text{ cm}^2\text{V}^{-1}\text{s}^{-2}$  for inorganic semiconductors.

### 1.2.2 Optoelectronic Polymers

Along with the electronic properties, conjugated polymers also exhibit unique optoelectronic properties in response to incidence of light. A wide variety of devices e.g. organic photovoltaics [16] and light emitting diodes [18, 19] exploit these optoelectronic properties of organic semiconductors. Band gap ranging from 1-3eV ensures that these materials can be excited by visible-NIR photons. Further, large absorption coefficient coupled with sizable density of photogenerated carriers allows for fabricating thin, transparent and light-weight structures unlike silicon based devices.

When a photon is incident on an optoelectronic polymer, a bound electron-hole pair known as exciton is formed. There are three important parameters governing the fate of the excitons: binding energy, diffusion length and life time. In semiconducting polymers, exciton binding energies, diffusion lengths and lifetime ranges from 0.4 to 1 eV, 1-10 nm and 1-10 ns respectively [20].



Greater binding energies of exciton make them stable at room temperature since room temperature energy is comparatively low. In order to facilitate the dissociation of individual charges, a blend of electron/hole acceptor and donor molecules is used. Driving force for the electron transfer from donor to acceptor is provided by the difference in lowest unoccupied molecular orbital energies (LUMO) of the donor and acceptor molecules. This is also evident from the energy level diagram shown in Figure 1.2.

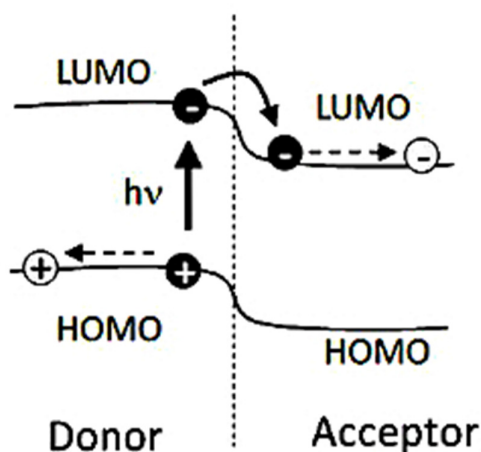


**Figure 1.3 : Energy level diagram for a bulk hetero junction system, photo-excitation and charge diffusion toward electrodes.**

Owing to the small exciton lifetimes, charge separation in the organic semiconductor should be very fast. Further, to address the issue of low diffusion lengths, donor and acceptor molecules are mixed at nanometer scale to form the bulk heterojunction system (BHJ)[21-23]. In BHJ system, there is always a surface available within the diffusion length scale where donor and acceptor materials coexist in a phase separated network composite. This enables the charge separation at the donor-acceptor (D/A) interfaces. However, there can be situations where the meta-stable electron-hole pair may still be coulombically bound and an additional

## Chapter 1

external electric field is required to facilitate the charge separation. In BHJ systems, charge separation happens in whole of the active layer due to presence of D/A interfaces throughout the layer. With the help of appropriate transport pathways from the interface to the respective electrodes, higher photon to electron conversion efficiencies can be achieved in BHJ based devices comparative to pristine or bilayered structure devices (Figure 1.3).

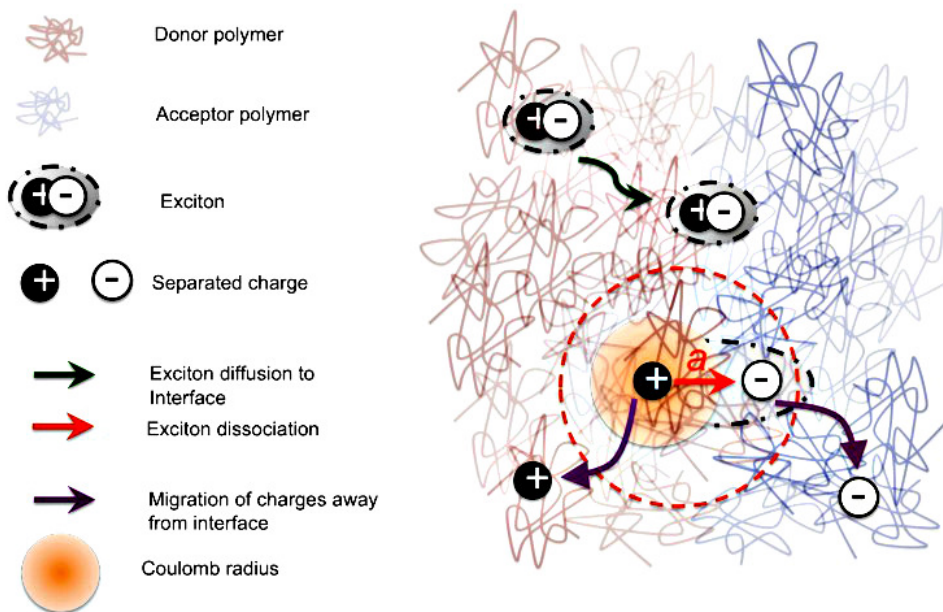


**Figure 1.4 : Charge separation at a donor/acceptor interface in a bulk heterojunction interface.**

Composition of BHJ, choice of electrodes and recombination losses are few of the parameters determining the photocurrents, photovoltages and incident photo to charge carrier efficiencies (IPCE). In one such approach, cathode is replaced by an electrolyte solution [24] which not only provides a valuable insight in understating the dynamics of transport processes but also represents a novel device architecture with potential applications in biological systems. Unique combination of electronic and optoelectronic properties in organic semiconductors is the basis for

many novel applications in the field of biointerfaces, working in the physiological environments.

Next few sections present a brief overview of the biological counterpart relevant to this report, namely; neurons, their functionality and retina.

### 1.3 Electrical Processes in Neurons

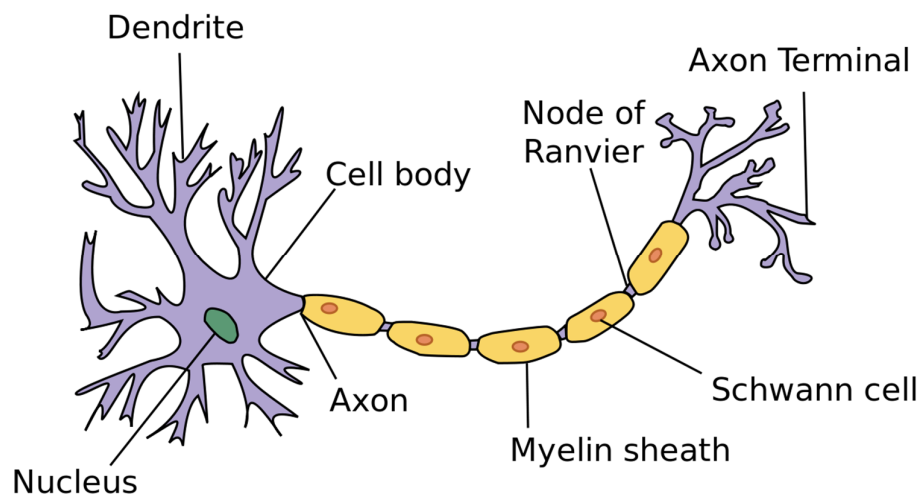


**Figure 1.5: Structure of a typical neuron**

Neurons are the basic functional and structural unit of the nervous system. Neurons transfer countless bits of information from various sensory organs to brain and vice versa. There are approximately  $10^{11}$  neurons present in human brain which are connected to each other as well as to the neurons in the peripheral nervous system to give rise to intricate neuronal networks. The junction at which one neuron is connected to the other is called a synapse. Though sensory neurons, like the one present in retina, are modified according to their function, still the basic architecture of neurons remains the same which is shown in the Figure 1.5.

## Chapter 1

Neurons consist of two main parts: soma or cell body and branches or neurites. Neurites are further of two kinds: dendrites and axons. Dendrites receive the signal from other neurons and pass it to the next neuron through axon. Thus, flow of information is unidirectional in neurons. Information is transferred in the form of electrical signals within the neurons and in the form of chemical signals between the neurons. Neurotransmitters are the biomolecules which carry the signals across the synapse.

A neuron responds to the external stimuli in the form of rapid changes in its membrane potential i.e. potential difference across the cell membrane. These rapid changes in potential difference are mediated by various types of ion channels. Ion channels are the special class of intrinsic proteins spanning the complete cross section of plasma membrane. Ion channels open or close in response to external stimuli and hence control the flow of ions across the plasma membrane by changing its permeability. Ion channels are extremely selective to ions and allow specific ions to pass through them. For example, there are ion channels specific for sodium and potassium ions [25].

### 1.3.1 Action Potential

Action potential or firing event is an all-or-none phenomenon exhibited by neurons in response to external stimuli. While travelling along the axon, action potential attenuates due to passive properties of neuronal membrane. However, action potential is regenerated when signal travels from one neuron to the next.

At rest, the potential difference across the neuronal cell membrane is approximately  $-70\text{mV}$  to  $-60\text{mV}$ . External stimuli decrease this potential difference

beyond the threshold potential ( $\sim -50\text{mV}$ ) and force the voltage gated  $\text{Na}^+$  channels to open.  $\text{Na}^+$  starts moving inside the cell due to concentration gradient. This makes the depolarization phase of an action potential as shown in Figure 1.6. Once this membrane potential becomes sufficiently positive,  $\text{K}^+$  ion channels open and an outward flow of  $\text{K}^+$  ions start rebuilding the negative potential difference across the cell which is called the repolarisation phase.  $\text{Na}^+$  ion channels get closed during the repolarization phase.

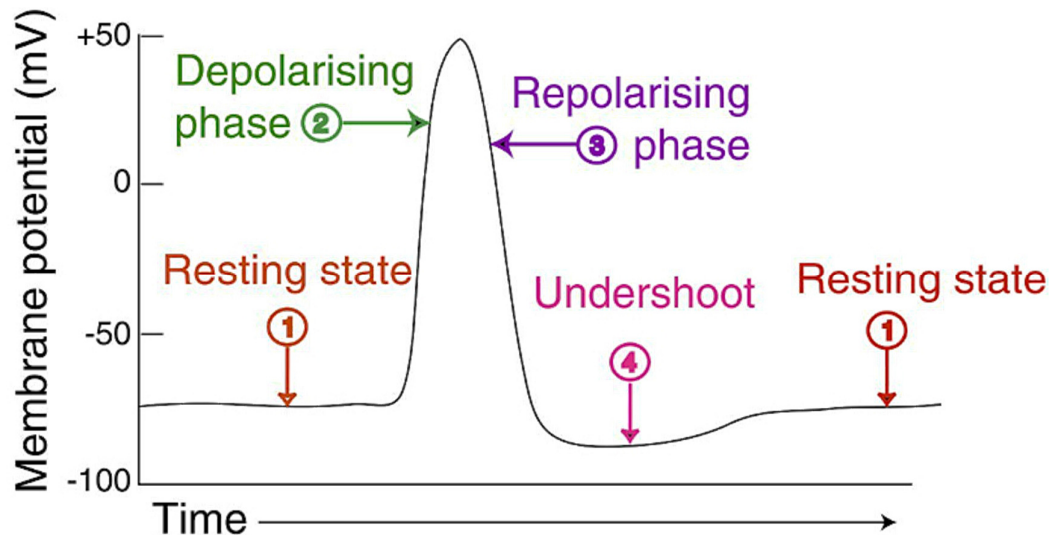


**Figure 1.6: Schematic showing course of action potential with time**

$\text{K}^+$  ion channels are slower comparative to  $\text{Na}^+$  ion channels so repolarization phase is slower than the depolarization phase.  $\text{K}^+$  ion channels have longer lifetime and hence make the cell hyperpolarized due to greater efflux of positive charge in the form of  $\text{K}^+$ . At this instance, energetically active  $\text{Na}^+/\text{K}^+$  pumps starts working to maintain the balance of ions on both the sides of the membrane to reach the resting potential again. Series of all these steps form an action potential [25].

## Chapter 1

The typical time span for an action potential is 1 to 5ms. Once the action potential is fired, a neuron cannot fire another action potential for some small interval of time which is called refractory period.

### 1.3.2 Recording Techniques

Recording electrical signal from excitable cells like neurons started in the 18<sup>th</sup> century itself when Galvani first observed that application of an electric pulse to a frog's nerve results in a twitch in the leg muscles. Presently, the branch of neuroscience dealing with recording these signals is known as electrophysiology. There are many techniques available to record the electrophysiological signals from the excitable cells like muscles, heart muscles and neurons. In the beginning, micron sized electrodes were used for intracellular as well as extracellular to record from the squid's giant axon. Hodgkin and Huxley used microelectrodes in voltage and current clamp mode to deduce their famous Hodgkin-Huxley equations for which they were awarded Nobel Prize in 1963. Another recording method called patch clamp was invented by Neher and Sakmann in 1976 which made it possible to record from a single open channel in cell membrane. However, both the techniques have limitations in terms of recording from multiple neurons arranged in three dimensional geometry simultaneously. To circumvent this issue, new devices called multielectrode arrays (MEA) are developed in the recent past. MEA consists of a large number of micron sized electrodes on a small transparent substrate enclosed in a chamber in which cells can be cultured directly. Each electrode is connected to a voltage amplifier, a series of filters and finally a computer to obtain the electrophysiological signal. Using MEA, electrophysiological signals can be

recorded with both temporal and spatial resolution. These recordings are done extracellularly which is why signal to noise ratio depends largely on the proximity of cells to the electrodes. Generally metal electrodes initiate apoptotic reactions and induce toxicity while in contact with cells. Organic semiconductors appear as promising material candidates for fabrication of soft electrodes with inherent biocompatibility. Optoelectronic properties of organic semiconductors further add the advantages of optical stimulation instead of electrical stimulation. Optoelectronic polymers can be directly interfaced with the neurons in the form of thin films or nanoparticles. This gives these materials an upper hand over other techniques of optical stimulation like optogenetics which involve tedious and elongated procedures of genetic engineering and protein expression.

## 1.4 Retina

Visual system receives light signals from the environment and converts it to the electrical signals which are taken to the brain and analyzed for perception of vision. Retina is the important multilayered sensory organ present at the back of eye which transduce the received light energy into electrical energy.

Retina consists of four major classes of neurons linked with each other intricately. The outermost layer is the photoreceptor layer containing rods and cones for intensity and color detection respectively. Diseases like retinitis pigmentosa (RP) and age-related macular degeneration (AMD) involve the malfunctioning of photoreceptors resulting in partial or complete loss of vision. Second layer from the outside is made up of bipolar cells. Rods and cones are connected to different bipolar cells and do not intermix.

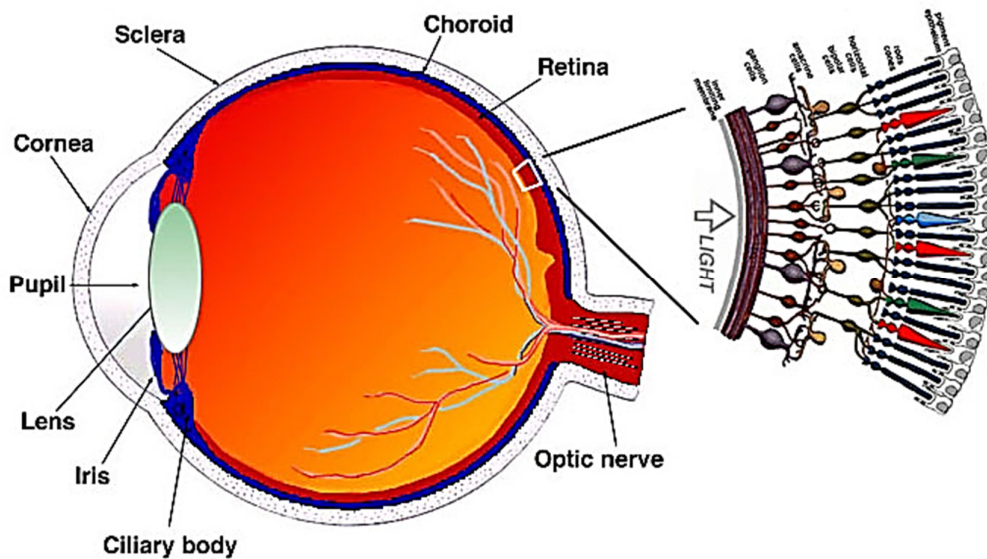


**Figure 1.7: Structure of human eye with inverted retina at the back and multilayered structure of retina**

Third layer is horizontal amacrine cells and the innermost layer is made of ganglion cells. Light signals are captured by the photoreceptors and converted to electrical signals which are carried to the ganglion cells and finally to the brain through optic nerve. Retina being a combination of both light sensitive photoreceptors and signal transducing neurons, provides one of the best platform for utilizing the optoelectronic materials for repair or augmenting the physiological vision mechanism.

In the subsequent chapters of this thesis, behavior in terms of stability and functionality of optoelectronic polymers is assessed when they are exposed to physiological conditions for a long time. To understand the effects of optoelectronic polymers on neurons, parameters like cell number, cytotoxicity, cell proliferation and neurite chatlength are monitored on different polymer substrates.



## CHAPTER 2

# **Long Term Stability of Polymer/Electrolyte Interfaces under Physiological Conditions**

### 2.1 Introduction

The chapter deals with the long term stability of polymer/electrolyte (P/EI) interfaces under physiological conditions. Degradation in P/EI interface is associated with electrochemical or light induced doping on the surface and formation of large number of trap states in the bulk. This eventually may result in attenuation in the magnitude of photogenerated potential which in turn may disrupt the functionality of such devices when integrated with biological systems. It has been shown recently that in P3HT, a charge transfer complex between polymer and molecular oxygen is formed when system is exposed to water or air for long time. The phenomenon is reversible in nature and this complex formation further get enhanced when system is illuminated with light [26]. However, there are very few reports about the long term stability of BHJ systems as a whole, especially under the complete physiological conditions and in contact with standard culture media as electrolytic solutions. Further, cell attachment factors like poly L-ornithine and Laminin may also affect the operational functionality of these interfaces, therefore it needs to be pursued and understood. As a consequence, long term stability of P/EI interfaces is targeted in this work. The measurements and evaluation is carried out using the magnitude of photogenerated transient spikes over long duration.

### 2.1.1 Semiconductor/Electrolyte Interfaces

Conventional semiconductors like silicon, germanium and GaAs are well known for their stable interfaces with electrolytes. Such interfaces are also extensively explored in literature given their use as electrodes in photovoltaic and catalytic cells [27-29]. Charge transfer reactions at the interfaces, excited electronic states, reactivity, surface corrosion, passivity, chemical sensing, impedance spectroscopy and electro-reflection are few of the key areas which have been investigated extensively in the past [30-35].

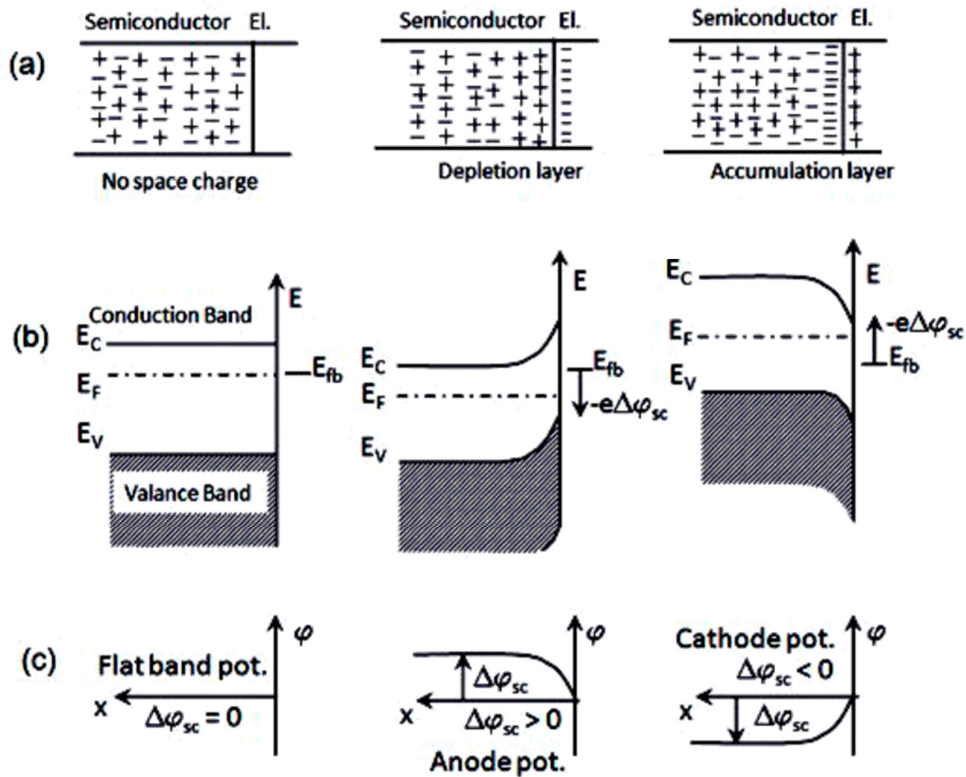


Figure 2.1: Schematic showing the space charge layers when n-type semiconductor is brought in contact with an electrolyte. (a) Distribution of charge carriers (b) Course of band edges (c) Course of electric potential. Redrawn from with permission [36].

Charge profiles, band diagrams and potential profiles for three typical situations that occur when a semiconductor is brought in contact with electrolyte are

shown in the Figure 2.1. When there is no space charge on the semiconductor, bands are flat and the potential is called flat-band potential. In case, when positive charge is present on the semiconductor side compensated with counter negative charges from the ions present in the electrolyte, a depletion layer lacking in electrons is formed on the semiconductor side. This results in bending of band edges downwards with respect to the interface. Similarly, in the case when depletion layer is negatively charged, band bending occurs in the upward direction. The layer of charges in the form of ions on the electrolyte side forms the accumulation layer.

In metal-electrolyte interfaces, excess charge on the metal side acts like a surface charge which get separated from ionic charge in the electrolyte by thin Helmholtz double layer. The complete structure can be considered as a capacitor and associated Helmholtz capacitance ( $C_H$ ). However, in case of semiconductor/electrolyte interface, diffuse space charge layer exists in semiconductors which adds another capacitance term. Depending on the conductivity between semiconductor and electrode, space charge capacitance can dominate the whole capacitance behavior of the interface.

### 2.1.2 Polymer/Electrolyte Interfaces

Organic semiconducting materials form unique interfaces when brought in contact with electrolyte solutions with very interesting properties. Many electrochemical processes occur at the P/EI interface. Charge transfer reactions and formation of electrical double layers are the most dominating processes. They have found applications in devices like polymer electrochemical photovoltaic cells and electrolyte-gated organic field effect transistors (OFETs) [37, 38]. Along with this,

## Chapter 2

P/EI interfaces also exhibit more interesting optoelectronic properties. Vini *et al* used the BHJ blend of P3HT and N2200 and showed a reversal in the photovoltage sign beyond a certain thickness of BHJ films on transparent ITO electrodes [39]. They also mentioned that, the P/EI system also provides an elegant system to study the mechanism of charge transport in such devices. In another report, a single pixel, single layer multicolor sensor is developed from the same BHJ system by exploiting the optoelectronic properties of P/EI [39] interface by the same group.

### 2.1.3 Polymer Based Biointerfaces

Electronic properties of organic semiconductors are extensively used in interfacing these materials with biological systems in tissue engineering [40], *in vivo* diagnosis of diseases [41-44] and controlled drug delivery [45]. Their inherent organic nature gives them an upper hand in biocompatibility which can be further improved by changing the substituents in the polymeric backbone. They exhibit ionic as well as electronic conductivities which render them one of the most suitable class of materials under physiological conditions. Thin films of these polymers are semitransparent which makes them compatible with many microscopic techniques. They self-assemble to mimic bio-structures and can direct cell differentiation[40]. Various indicator/enzyme/neurotransmitter molecules can be incorporated on the surface or inside the bulk of these materials which can be released in a controlled fashion by application of external stimuli like temperature, pH, magnetic and electric fields [46, 47].

However, the field of biological applications of optoelectronic properties of organic semiconductors is relatively new and unexplored. In addition to the direct

applications like neuroprosthetics for visual system, optoelectronic polymers also open the possibility of augmented vision extending the normal visible spectra. This is because of freedom to tune the absorption range of the polymers to any desired level. Further, optoelectronic properties can also be used for optical control of things occurring inside the polymer and in turn interfaced neurons. Ease of manipulating light beams with greater control and resolution to the advantage while using optoelectronic polymer as recording or stimulating electrodes.

## 2.2 Experimental Section

### 2.2.1 Experimental Strategy

Three important parameters were decided to be introduced in the environment in order to resemble it with physiological conditions: a) culture media instead of KCl as an electrolyte, b) 5% CO<sub>2</sub> environment around the device and c) raising the ambient temperature to a value equivalent to physiological temperature i.e. 37 °C. However, in the beginning, long term photoresponse was observed for BHJ/KCl interface. This was necessary to have a reference for knowing the degradation trends under non-physiological conditions since there are no reports available addressing the degradation over such a long duration of time. Also, this study has found importance in understanding the physical aspects like mechanism of degradation and role of wavelength, intensity and thickness in degradation over a long time.

Experiments were performed using different kinds of ground electrodes. In first case, a thin copper wire dipped in the electrolyte solution was used while in the second case, ITO/glass plates were used as counter ground electrodes. Use of copper wire gave the freedom to exchange the gases with the environment which was

## Chapter 2

necessary for second set of experiments about understanding the role of 5% CO<sub>2</sub> in the degradation. Though, it also allowed the electrolyte solution to evaporate as a side effect. Second approach of sealing the electrolyte chamber with ITO/glass plates was implied to stop the evaporation, however, it excluded the possibility of studying the effects of culture media and CO<sub>2</sub> simultaneously on the P/EI interface.

### 2.2.2 Materials Used

P/EI interface was fabricated using BHJ system and different electrolytes. P3HT and N2200 molecules were used as donor and acceptor molecules in BHJ system. P3HT was procured from Sigma Aldrich, and N2200 was obtained from Polyera ActivInk, USA. All the chemicals were used without any further purification. Figure 2.2 shows the structure, relative energy level diagram and absorption spectra for both the polymers. KCl and a standard culture medium, Dulbecco's Modified Essential Medium (DMEM) were used as electrolytes. Poly L-ornithine hydrobromide (Sigma Aldrich) and Laminin (Life Technologies) were used as cell attachment factors.

### 2.2.3 Device Fabrication

BHJ system was prepared by blending P3HT and N2200 in 4:1 weight ratio in chlorobenzene (Sigma-Aldrich). The blend was mixed using magnetic stirrer for at least 6 hours and final concentration was 10mg/mL. Indium Tin Oxide (ITO)

( $\sim 20\Omega/\square$ ) coated glass pieces of approximately 2 cm  $\times$  2 cm size were used as substrates. All the substrates were cleaned by the standard procedure which included ultra-sonication in soap, water, chloroform, isopropyl alcohol and acetone sequentially, each for a duration of 10 minutes.

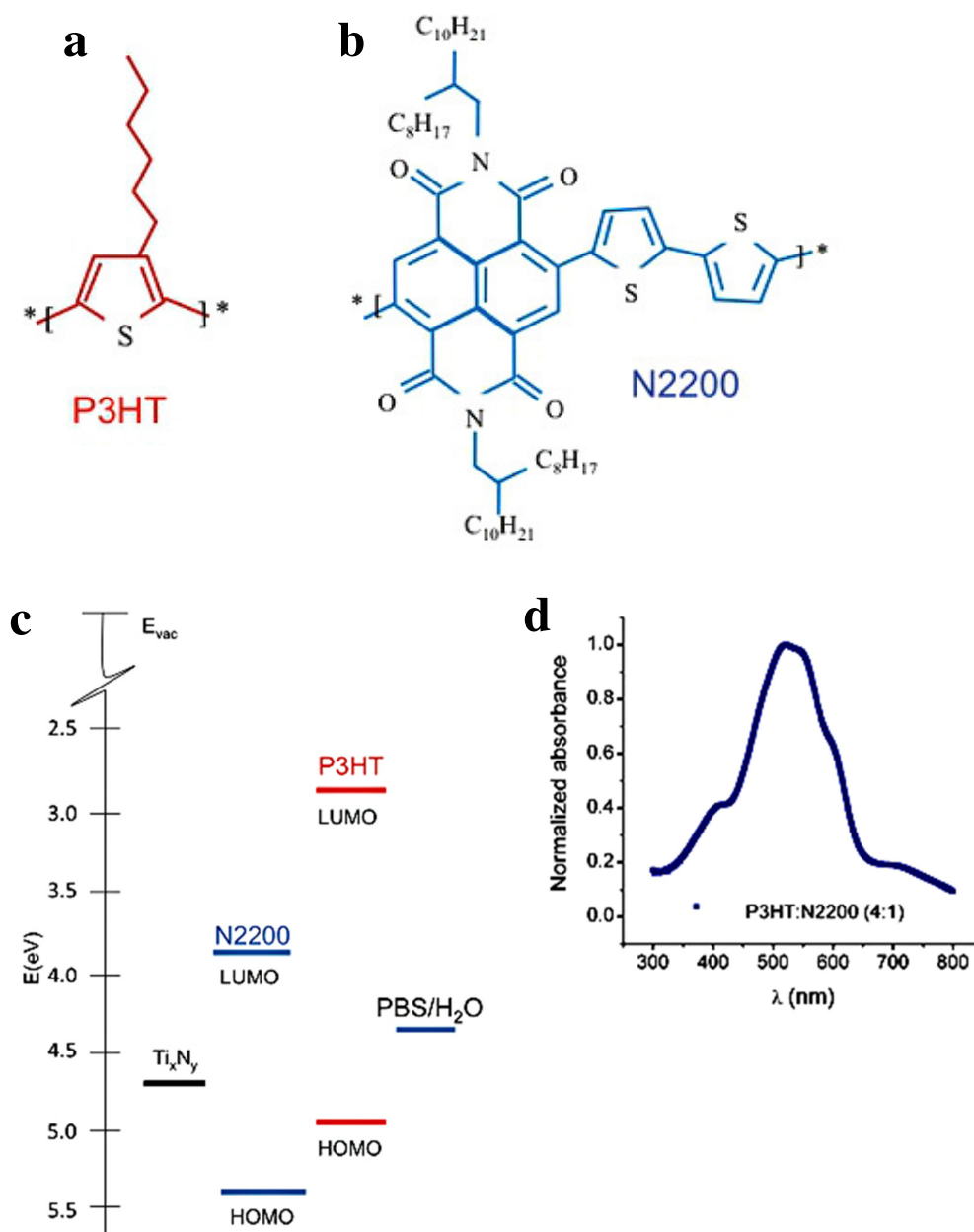


**Figure 2.2 :** Chemical structures of (a) P3HT, (b) N2200, (c) relative energy levels of P3HT and N2200 (d) and normalized absorption spectrum of BHJ consisting of P3HT and N2200.

## Chapter 2

On the cleaned substrates, thick (1-3  $\mu\text{m}$ ) films of BHJ were drop casted. After the solvent evaporation, films were annealed at 110°C for 10 minutes and then allowed to come on room temperature. All the steps involving use of polymers were performed inside the nitrogen filled glovebox (Mbraun Inc.). For electrolytes, 100 mM KCl (Sigma-Aldrich) solution was prepared. However, for DMEM (Sigma-Aldrich) culture media, commercially available formulas was used after addition of  $\text{NaHCO}_3$  (SRL Chemicals) as mentioned in the datasheet of the product. Poly-L-ornithine hydrobromide and Laminin were used in final working concentrations of 25  $\mu\text{g/mL}$  and 2  $\mu\text{g/mL}$  respectively. Precleaned ITO/glass plates and copper wires were used as counter ground electrodes. For holding the electrolyte solution over the BHJ, glass rings with diameter 1 cm and height 6 mm were used. Ring was sealed over the BHJ film using epoxy adhesive (Araldite), electrolyte was filled using a micropipette and ITO/glass plate (counter electrode) was sealed over the glass ring using ordinary grease. It was ensured that the electrolyte remain in the contact with the counter electrode with no air bubbles.

### 2.2.4 Photoillumination and Photovoltage Measurement Setup

BHJ/electrolyte (BHJ/EI) interface was illuminated from the electrolyte side. The experimental set up is shown in Figure 2.3. For photoillumination, red, green and blue colored LEDs (5 mm) were used. LEDs were mounted on 3D printed structure which held the LED at a fixed distance of 2 cm above the BHJ/EI interface. LEDs were driven by an Arduino Mega 2560 microcontroller board. For measuring transient spikes, an oscilloscope (Tektronix MSO 4054B) in DC (50  $\Omega$ )



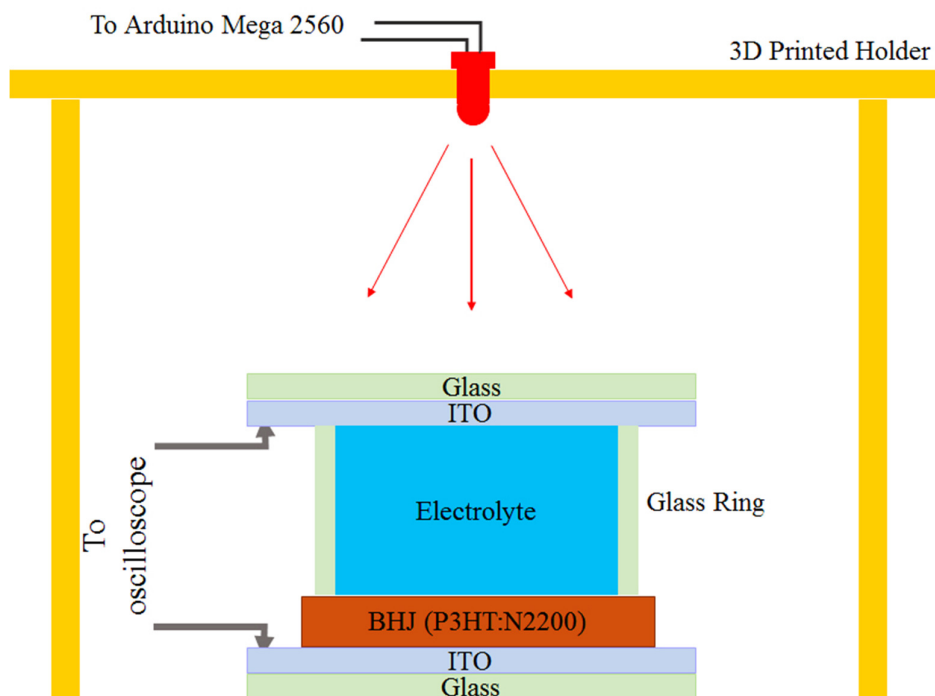
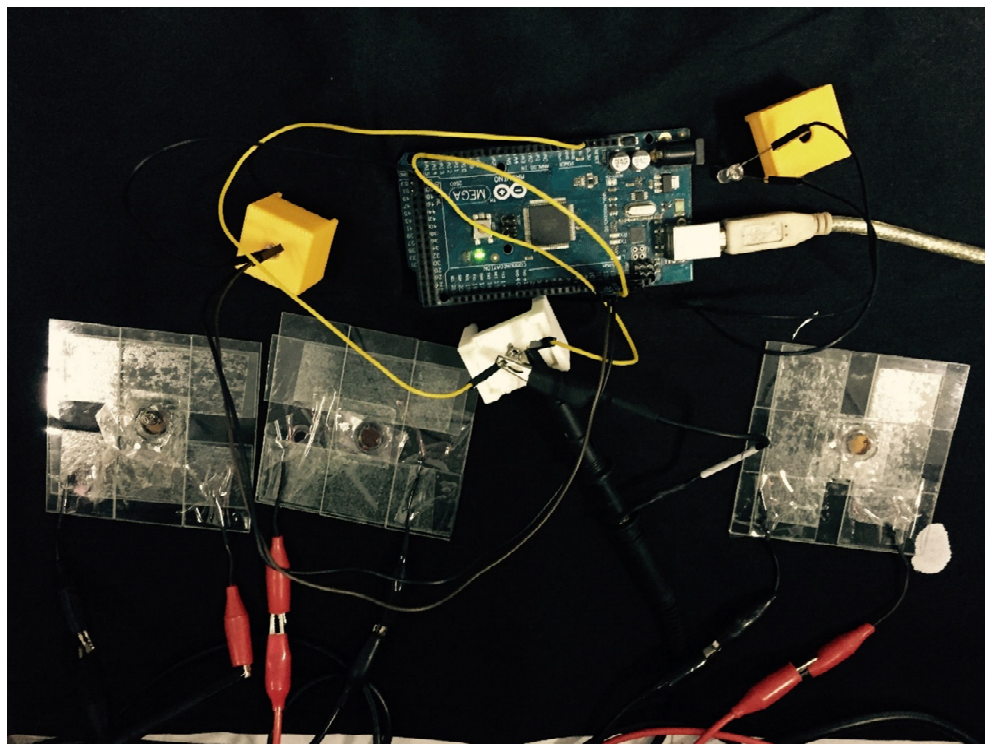


**Figure 2.3 : Schematic showing the experimental setup (Not to scale).**



## Chapter 2

coupling mode was used. Sampling rate was 50 samples/second while X and Y axis resolutions were set to be 2 s/division and 10 mV/division respectively. Whole of the setup including Arduino and oscilloscope was programmed and controlled remotely using a custom made program (attached in appendix) in LabVIEW (National Instruments). BHJ/EI interface was illuminated for 1 s after an interval of 10 s and photovoltage response was recorded. Recordings were done for duration exceeding 18 hours of operation.

### 2.3 Results

Figure 2.4 (a) shows the photovoltage profile obtained for three different samples from the same batch when illuminated with three different wavelengths of light. The emission spectra for three LEDs used is shown in the Figure 2.4 (b). ITO/glass electrodes were used for this set of measurements. BHJ/KCl interface exhibited transient response as function of wavelength as reported by Vini *et al* [39, 48]. A positive value of photovoltage was observed on incidence on green ( $\lambda = 453$  nm) light which changed polarity on incidence of red ( $\lambda = 644$  nm) light. This unique ability to reverse the polarity is the basis for multicolor detection using single pixel and single layered optoelectronic devices as previously shown by Vini *et al*[4]. For all three wavelengths, photovoltage shows a maxima or minima on onset or offset of square light pulse. To observe the long term response, similar datasets were recorded after every 10 s and the maxima and minima were plotted with respect to time which is shown in the Figure 2.5 and 2.6.

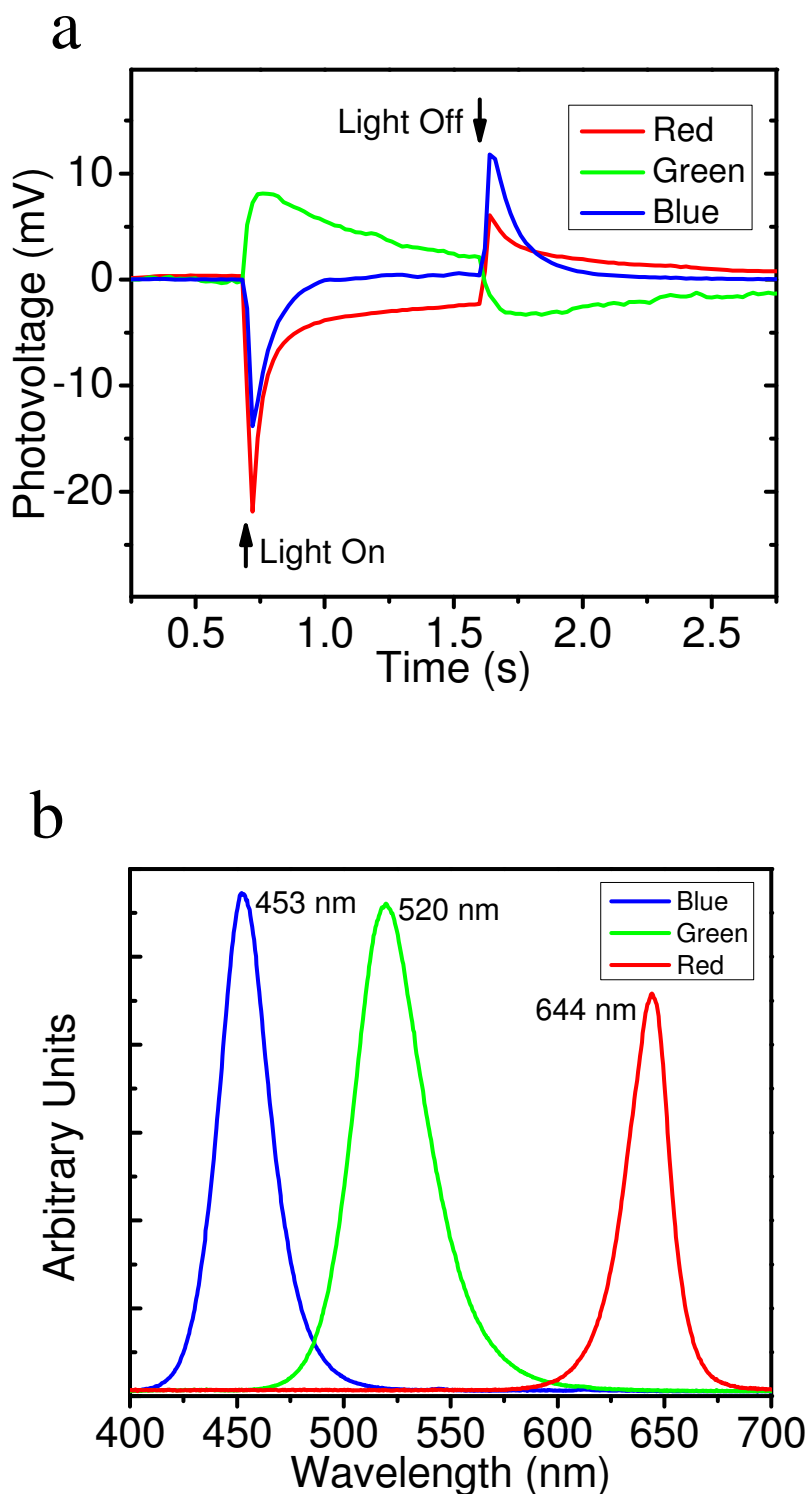


**Figure 2.4:** (a) Photovoltage profile for BHJ/electrolyte device when illuminated with LEDs of different color, (b) Emission spectra for different LEDs.

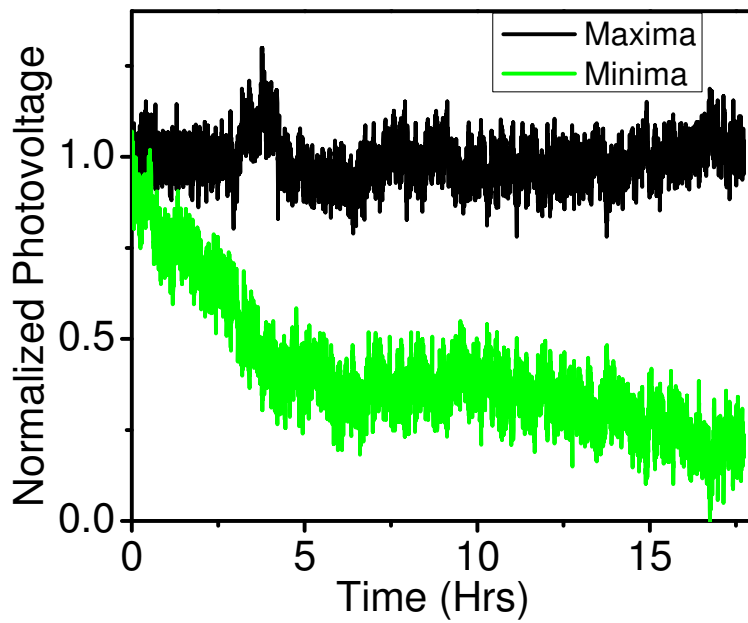
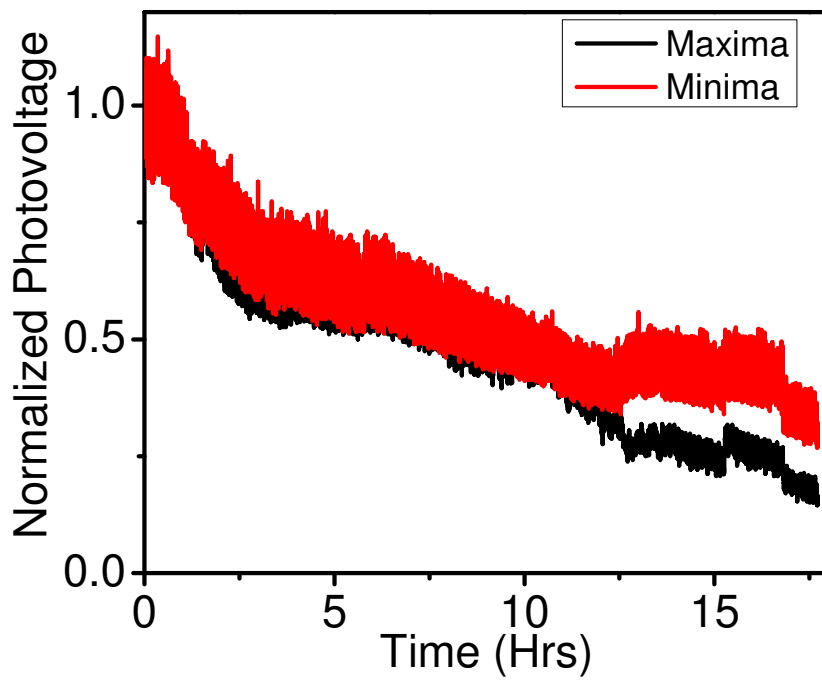


**Figure 2.5: Long term normalized ( $V_{\text{peak}}/V_{\text{peak at } t=0}$ ) response of maxima and minima for (a)  $\lambda = 644$  nm and (b)  $\lambda = 520$  nm**

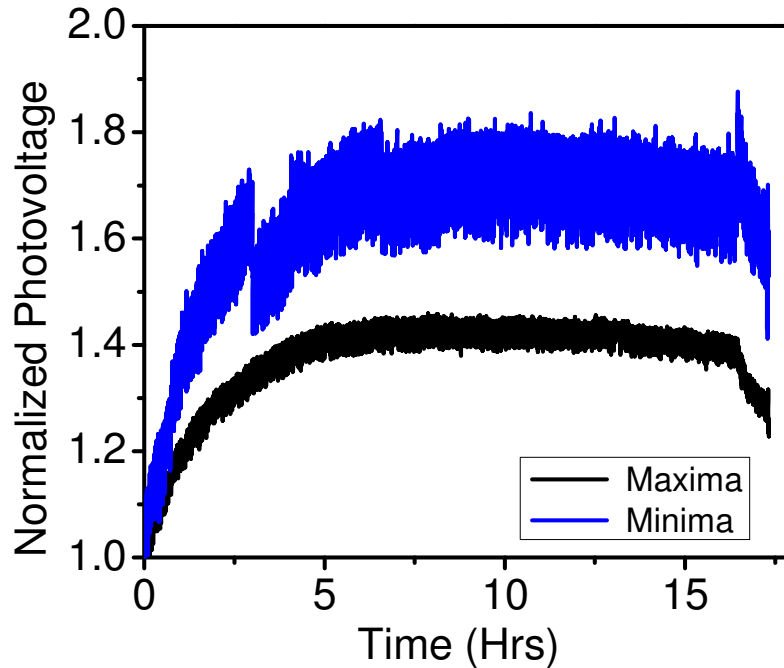


**Figure 2.6 : Long term normalized ( $V_{\text{peak}}/V_{\text{peak at } t=0}$ ) response of maxima and minima for ( $\lambda = 453 \text{ nm}$ )**

Noteworthy points in Figure 2.5 and 2.6 are the following:

- i. Magnitude of both the maxima and minima decreases by 80% with time in case of illumination with  $\lambda = 644 \text{ nm}$ .
- ii. Magnitude of maxima is relatively unchanged in case of  $\lambda = 520 \text{ nm}$ , however, the minima reduces by  $\sim 75\%$ .
- iii. Magnitude of both the maxima and the minima increases by 40% and 70% respectively for  $\lambda = 453 \text{ nm}$  and gradually saturates to a stabilized value.

In all the three cases with different wavelength for photoexcitation, the profiles for maxima and minima are relatively similar.

## 2.4 Discussions

The pulsed response with characteristic polarity has been explored for color discrimination procedure without the need for filters and dispersing elements in the optics [39]. The origin of reversal in polarity of transient response in ITO/BHJ/EI based devices can be understood in terms of differences in the rate of carrier accumulation at the BHJ/EI and ITO/BHJ interfaces. Thickness of BHJ layer and absorption coefficients for the incident light are crucial parameters, deciding the color discrimination characteristics of such devices. In case of illumination from the electrolyte side with low absorption (Figure 2.4a) at  $\lambda \sim 644$  nm, generation of photoinduced charges is more likely to happen closer to the ITO/BHJ interface considering the larger penetration depth. This results in the accumulation of excess negative charge carriers at the ITO/BHJ interface and negative polarity in transient response. It should also be noted that N2200 has a tendency to form organized microstructures [49, 50]. A predominant network of acceptor molecules near the ITO/BHJ interface may further facilitate the accumulation of excess negative charge carriers. In case of high absorption  $\lambda$  ( $\sim 453$  nm), positive value of photovoltage is observed in transient spike. It is also being shown that using a selective back reflector, BHJ/EI devices can also be used for differentiating all three primary colors, where the action of blue light on the device can be considered as a combined action of red and green light. Our results show that sum of photovoltages observed for red and green show similar profile as blue which is shown in Figure 2.7.

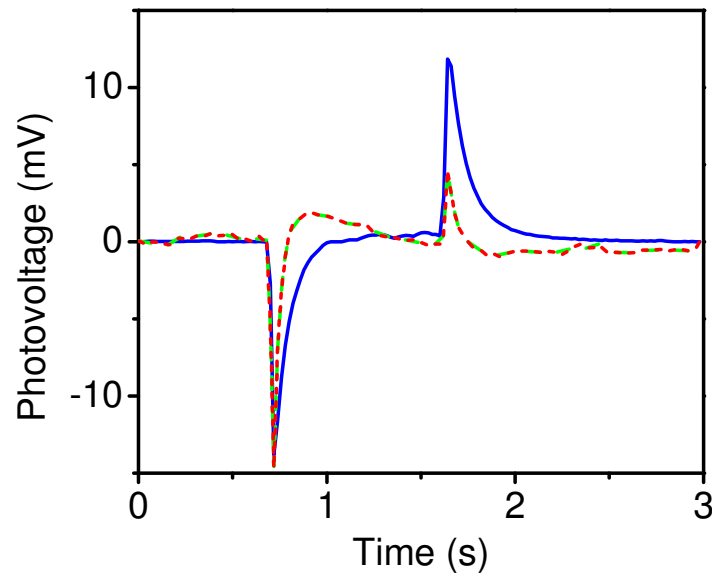


**Figure 2.1 : Comparison between blue and curve obtained from summation of red and green**

From the long term results, it is observed that the degradation process is a function of wavelength of illuminating light. It is known in case of BHJ/Electrolyte devices that constant illumination causes the accumulation and recombination of charge carriers which eventually results in reduced photoresponse. The observed similarity between the maxima and minima profiles for a specific wavelengths indicates that the events responsible for transient behavior either follow exactly the same mechanism or at least occur at the same interface. It is also possible that every cycle of illumination deposits small number of ions on the interface which blocked the light from falling on to the BHJ/El interface eventually. To draw a conclusion about the mechanism governing these changes in photovoltage over such a long duration, further investigation is in progress. Also, experiments related to physiological conditions are in progress.





## CHAPTER 3

# Optoelectronic Semiconducting Polymers as Active Biocompatible Interfaces for Neuronal Cells

### 3.1 Introduction

The innovation in biomedical implants always strive for novel materials with versatile functionality and biocompatibility. One of the biggest challenge in the field is interfacing these materials with the biological systems without making a compromise between the functionality of either the biological system itself or the implants. Mostly, interfacing a material with a tissue or organ initiates a complex series of reactions which can evoke the release of chemotactic and growth factors or start inflammatory responses. Research about novel materials for biomedical implants tries to minimize these unwanted responses. Surface modifications to overcome nonspecific protein adsorption and precision immobilization of signaling group on the surfaces are few of the commonly used strategies to avoid inflammations.

Conjugated polymers like PEDOT:PSS has already been utilized for developing biosensors, neuronal probes and active substrates for tissue engineering [40, 49, 51-53]. Recently, optoelectronic polymers are also interfaced with live retinal tissues in BHJ as well as pristine configuration [4, 12]. These early results indicate many promising possibilities, as well as have raised many questions. In this

## Chapter 3

chapter, the question about the effects of the P3HT, N2200 and BHJ system on neuronal systems has been addressed. Number of cells, cytotoxicity, proliferation and neurite length are the key parameters which can give information about the biocompatibility of the optoelectronic polymers. Also, taking into account the optoelectronic properties of polymers, effects of light illumination on proliferation and neurite lengths are also monitored.

### 3.2 Experimental Section

#### 3.2.1 Materials Used

Organic semiconductors: P3HT and N2200 were used for this work. Two immortal cell lines 1) SH-SY5Y (ATCC) of human neuroblastoma origin and 2) U87-MG of human glioblastoma origin were utilized. Both of these cell lines have neuronal origin. As a consequence, these are of particular interest for this study about polymer-neuronal interface. Along with these, retinal neurons were also extracted and utilized from a primary source BALB/c mice pups within 0-2 postnatal days.

#### 3.2.2. Fabrication of Polymer Thin Films

In order to address the biocompatibility, aforementioned cells were cultured on polymer thin films. Thin films (200-400 nm) were prepared by spin coating the P3HT, N2200 and BHJ blend solutions on the substrates at 1000 rpm speed for 60 s. Glass coverslips of diameter 18 mm were used as substrates after cleaning

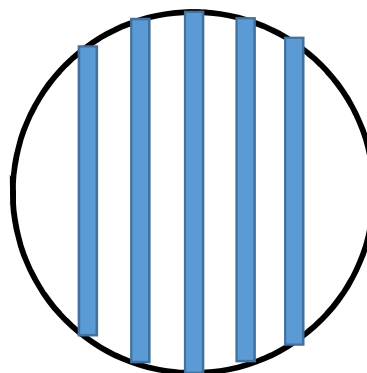


**Figure 3.1 : Patterning the polymer strips on cover slip. Polymer is shown in blue.**

through the standard procedure as explained in the earlier chapter. Cleaned glass cover slips without the polymer were used for control experiments. In some of the samples, polymer films were patterned in parallel strips by physical masking (Figure 3.1). Spin casted films were annealed at 110°C for 10 minutes and allowed to cool till room temperature. All the steps involving use of polymers were performed inside the moisture and oxygen free, nitrogen filled glovebox (Mbraun Inc.).

### 3.2.3 Sterilization of Polymer Films for Cell Culture

For sterilizing the polymer films, a sequential combination of 70% ethanol and UV light exposure was used. Initially, all the samples were rinsed in 70% ethanol for 10 minute followed by exposure to UV light for 10 minutes inside the vertical laminar flow unit. After this, cover slips were transferred to pretreated 12-well culture plates (Nunc) and washed with 70% ethanol. In the next step, three consecutive washes with phosphate buffer saline (PBS) were given followed by exposure to UV light for another 20 minutes. This completed with the sterilization of polymer films.

### 3.2.4 Ornithine/Laminin Treatment

For adherence and proliferation, the polymer films were treated with poly-L-ornithine and extra-cellular matrix protein Laminin in layer by layer self-assembly. Both of these coatings are known to promote cell adhesion and proliferation of neuronal cells in culture [54, 55]. The working concentration of L-ornithine (Poly-L-ornithine hydrobromide from Sigma Aldrich) and Laminin (Laminin from Engelbreth-Holm-Swarm (EHS) sarcoma of mouse origin, Life Technologies) were 25 µg/mL and 2 µg/mL in PBS respectively. The sterilized substrates were incubated

## Chapter 3

in ornithine solution for 6 hours followed by one wash with PBS and again incubated in Laminin solution for another 6 hours. Before plating the cells, the ornithine/Laminin-coated substrates were washed with PBS thrice. This procedure was carried out inside the laminar hood and all aseptic precautions were taken to avoid contamination. All the further protocols described below were also carried out under similar sterile conditions.

### 3.2.5. Preparation of Immortal Cell Lines

Immortal cell lines SH-SY5Y and U87-MG were maintained in fresh DMEM and EMEM media respectively, both supplemented with 10% Fetal Bovine Serum (FBS) obtained from Gibco, Life Technologies. Cells were incubated at 37 °C in a 5% CO<sub>2</sub> filled humid chamber. A mixture of antibiotics 1% penicillin-streptomycin was also added to the media. Cells were dissociated with 0.25% trypsin and 0.05 mM EDTA solution and plated on a new culture dish or polymer thin films after they reached 70-80% confluency. On polymer thin films, cells were seeded at a density of  $\sim 5 \times 10^4$  cells/cm<sup>2</sup>. Cell viability was checked using trypan blue staining. Every experiment was performed in triplicate with three separate control experiments. Bright field microscopic images were acquired after approximately 36 hours using an inverted light microscope (Olympus Legends IX 7) equipped with a color CCD camera for further analysis.

### 3.2.6 Extraction of Primary Retinal Cells

Retinas were isolated from BALB/c (P0-P2) mice strains without any preference to gender. Mice pups were euthanized by overdose of halothane vapors followed by enucleation of eyes. Further procedure was performed under the dissection microscope in Earl's Balanced Salt Solution (EBSS) medium. Eyes were

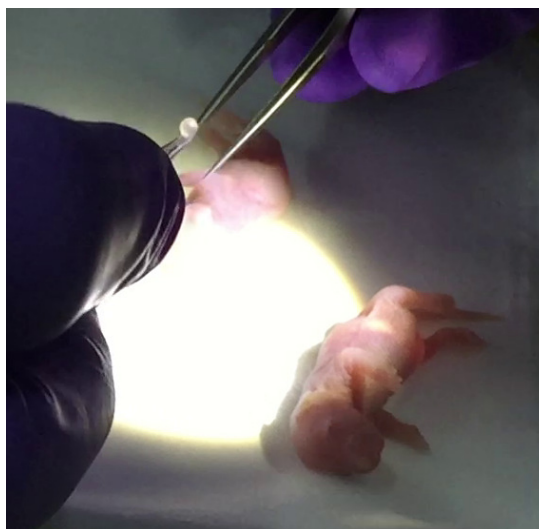


**Figure 3.2: Enucleated eye from a mice pup**

punctured using forceps and white retinal tissue was separated. The tissue was dissociated in 1 mL EBSS solution consisting of 50  $\mu$ l of papain (400 U/mL), activated with 1 mM L-cystein and stabilized with 0.5 mM of EDTA. Dissociated cells were triturated in a 1 mL solution of EBSS containing 50  $\mu$ l of DNase I (2000 U/mL), 5  $\mu$ g/mL of leupeptin and 1% Bovine serum Albumin (BSA). The cell pellet was resuspended in the DMEM culture medium supplemented with 4% fetal bovine serum, 1% N2 and 1% B27 supplement, 1% penicillin-streptomycin, and 1% glutamine. Cell density was counted using a haemocytometer and was typically  $\sim 10^6$  cells/mL. The culture medium was replaced every 2<sup>nd</sup>-3<sup>rd</sup> day during the growth. Images were captured on 15<sup>th</sup> day for analysis. For primary cells also, every experiment was performed in triplicate with three control experiments.

### 3.2.7. Photoillumination Setup

For photoillumination of the substrates during the cell culture, an assembly of blue and red LEDs were fabricated in the lab. The LEDs were mounted on a printed circuit board with spacing equal to the well-to-well spacing in the 12-well plate. The LEDs were driven using a microcontroller Arduino MEGA 2560 board, which was placed inside a box on. A 3D printed structure was also designed to hold the culture plate in place while illumination. Photoillumination was achieved from the ITO/polymer side with a pulse width of 1 s and a pulse interval of 1 s. A snapshot of this assembly is shown in Figure 3.3.. The photoillumination was started after 24 hours of cell plating and was carried out for 6 hours every day while cells were in culture.

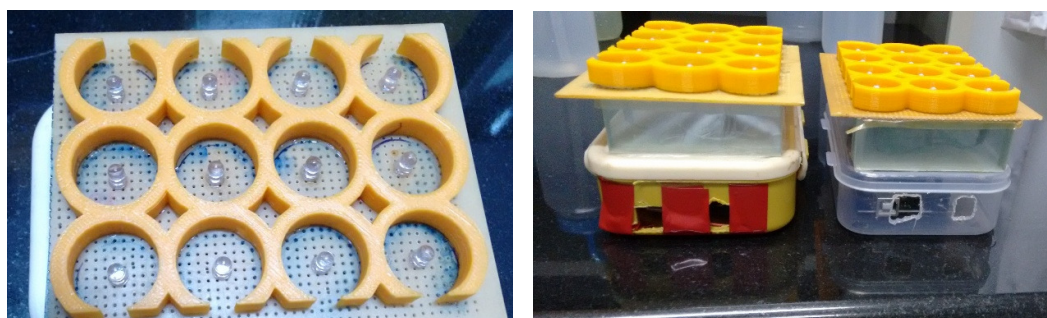


**Figure 3.3 : Photoillumination assembly for studying the effects of light. 3D printed culture plate holder is shown in yellow.**

### 3.3 Observations & Analysis

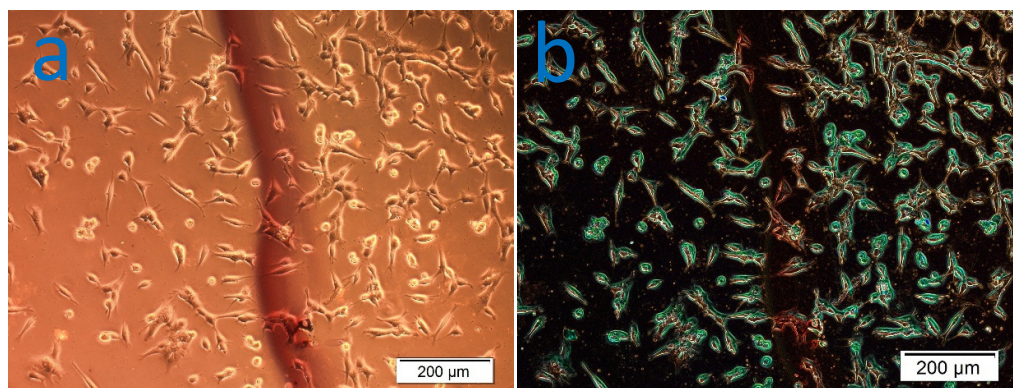
Cells were imaged after 36 hours of cell plating for immortal cell lines and 15-20 days for primary retinal cells using bright field microscopy. For samples in which, polymer films and glass coexist, it was taken care while imaging that in each image

both the polymer substrate and glass substrates should be observed. Six images from each sample culture well were captured at randomly selected places.

From these images, cell density on polymer and glass substrates were calculated for the sample culture well containing both polymer covered area and glass. For control experiments, cell density was measured in the complete image. Olympus cellSens program was used for image analysis. Direct cell counting algorithm of was found to be ineffective on the direct images without any processing. This may also be due to coexistence of polymer and glass surfaces in the same image which resulted in different contrast in the different regions in the image. In order to count the cells, first edge detection was performed in each image using Sobel algorithm followed by determination of cell density on a randomly selected largest possible area on polymer as well as glass side.

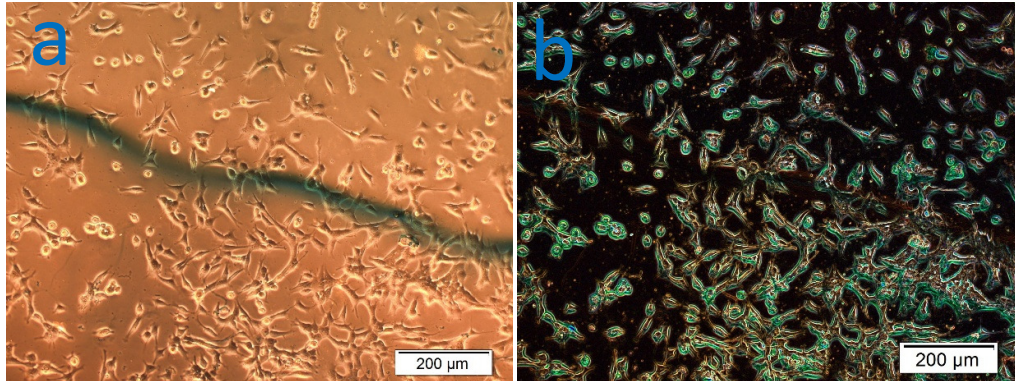
### 3.4 Results & Discussions

Growth of SH-SY5Y cells on the P3HT substrate are shown in the Figure 3.4. The region having the polymer film appears darker in comparison to glass as visible in Figure 3.4 a. Difference in cell density between polymer substrate and glass substrate

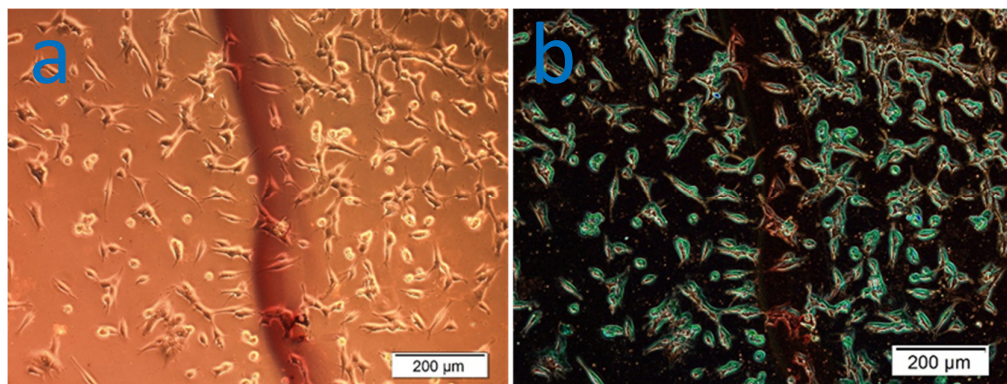


**Figure 3.4 : (a) Microscopic image of growth of SH-SY5Y cells on P3HT substrate, DIV 2, (b) Same image after edge detection. Difference in cell density is clearly evident in this image.**

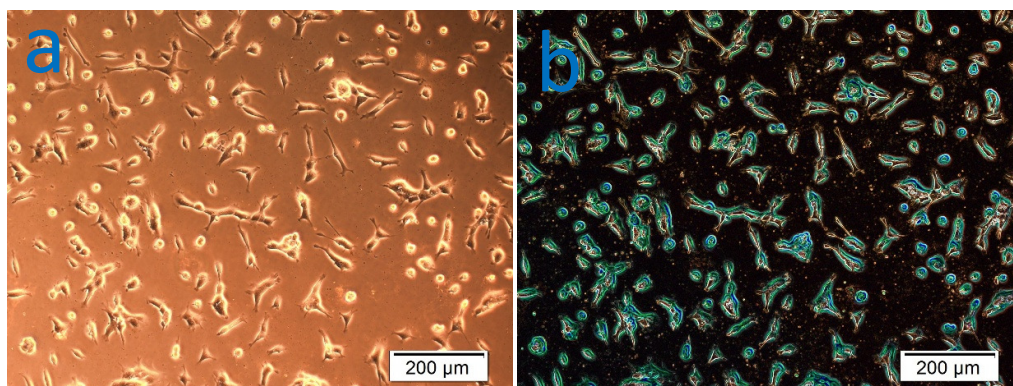
is clearly evident in the processed image after detecting the edges. Similarly, SH-SY5Y cell lines are shown in on other substrates are shown in Figure 3.5 and 3.6.



**Figure 3.5: (a) Microscopic image of growth of SH-SH5Y cells on N2200 substrate, DIV 2, (b) Same image after edge detection.**



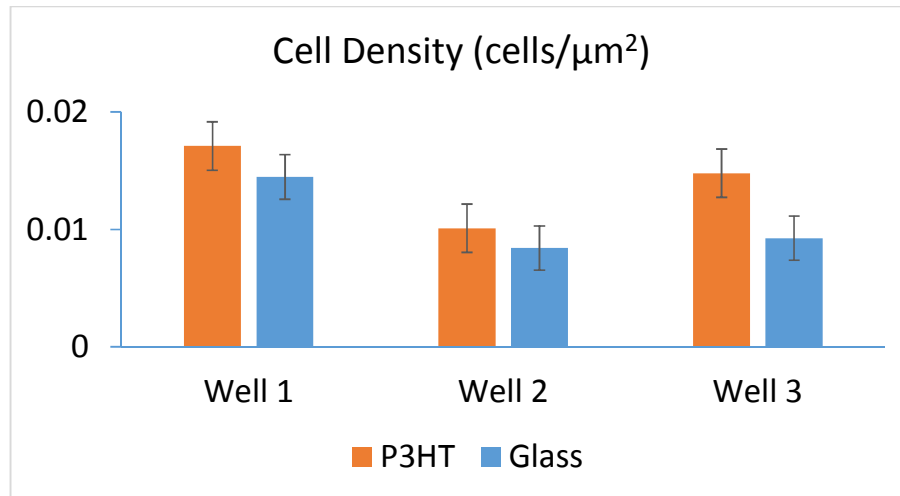
**Figure 3.6: (a) Microscopic image of growth of SH-SH5Y cells on polymer blend (P3HT: N2200) substrate, DIV 2, (b) Same image after edge detection.**



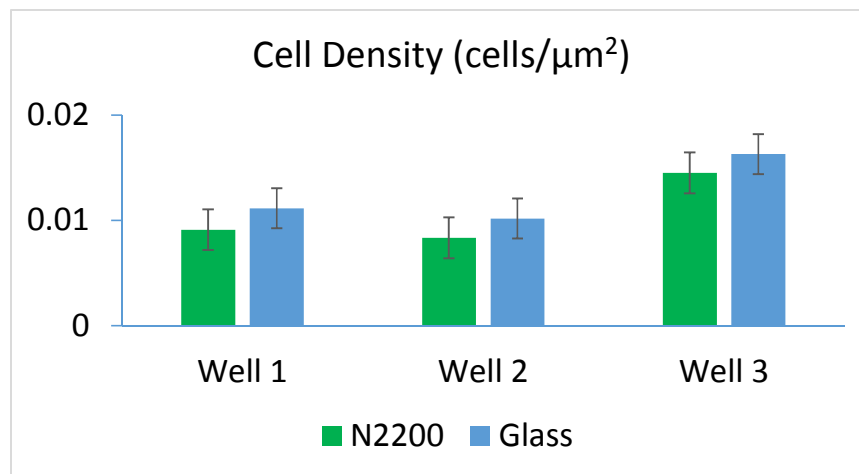
**Figure 3.7: (a) Microscopic image of growth of SH-SH5Y cells on glass substrate for control experiments, DIV 2, (b) Same image after edge detection.**



Figure 3.7 shows the control experiment without any polymers film in the culture well. Cell density from the all the six images was averaged for all three culture wells and shown in Figure 3.8, 3.9 and 3.10 for P3HT, N2200 and BHJ system respectively.



**Figure 3.6 : Histogram showing cell density comparison for P3HT and glass regions coexisting in the same well. Data are shown in mean + standard error in mean (SEM) configuration for the six images from the same well.**



**Figure 3.7 : Histogram showing cell density comparison for N2200 and glass regions coexisting in the same culture well. Data are shown in mean + standard error in mean (SEM) configuration for the six images from the same culture well.**

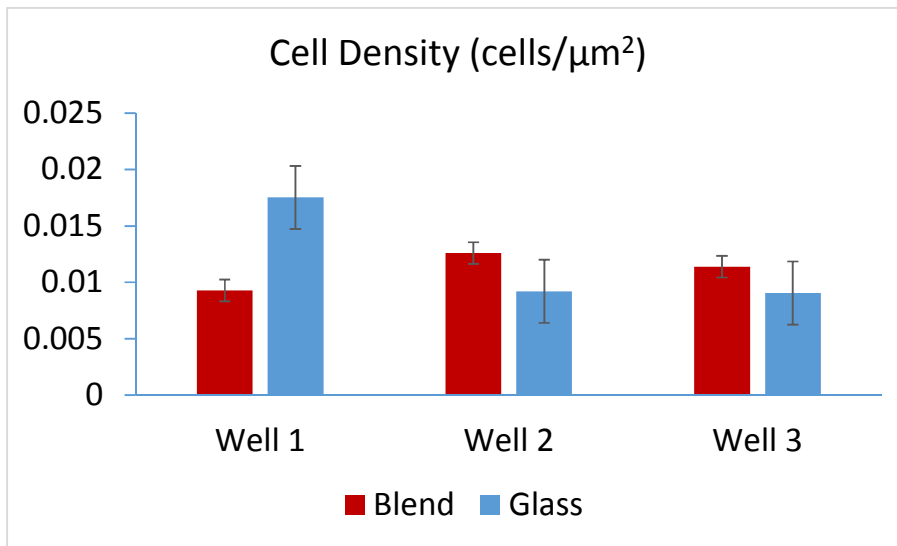


**Figure 3.8:** Histogram showing cell density comparison for Blend system and glass regions coexisting in the same culture well. Data are shown in mean + standard error in mean (SEM) configuration for the six images from the same culture well.

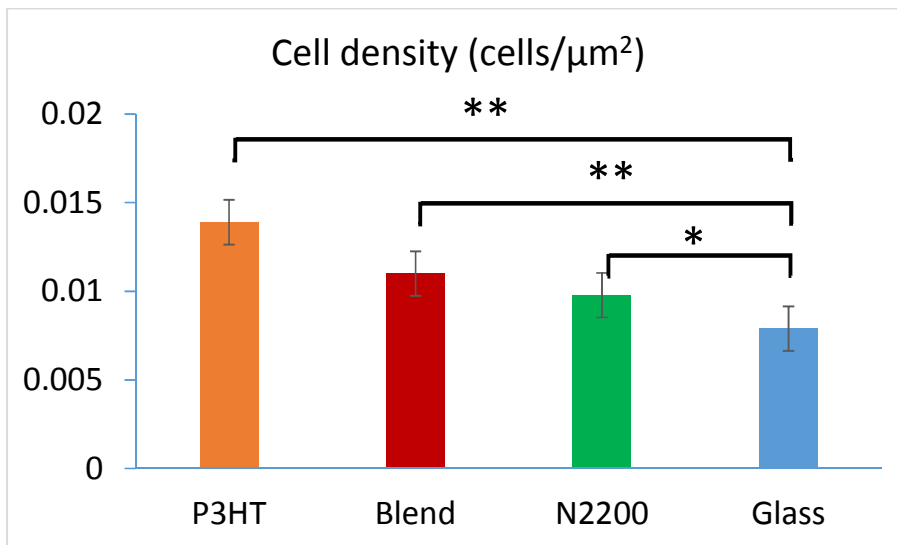


**Figure 3.9 :** Histogram showing comparison among cell densities in P3HT, N2200, Blend, N2200 and glass (control) experiments. Data are shown in mean + standard error in mean (SEM) configuration. \*Significance against glass at p < 0.05, \*\*Significance against glass at p < 0.02. (ANOVA test)

All the experiment shown here were performed in dark. In P3HT and BHJ systems, slight increment in the cell density is observed. Increment is found to be consistent in all three culture wells in the case of P3HT. However, in case of BHJ system, reverse trend is observed. For N2200, a decrease in cell density is observed consistently in all three culture well. The results were found to be in agreement for P3HT with the literature [52, 56, 57]. However, there are very few reports about biocompatibility of N2200. P3HT in pristine state [12] as well as BHJ configuration [4] was shown to elicit action potentials in retinal neurons in earlier reports also by forming a close contact with the neuronal tissue. Figure 3.11 shows a very interesting result where cell density is found to be increased in comparison to the control experiments, in statistically significantly magnitude (ANOVA test). It is evident that polymer substrates provide better opportunities for growth of neurons comparative to glass substrates. This proves their potential for future neuroprosthetic implants. The difference in the results, when cell density is compared with respect to glass substrate in the same culture well and glass substrate in a completely different culture well (control) indicates that there may be a chemical cue released by the polymer in the physiological media. This resulted in the enhanced rates of cell proliferation on the glass surfaces present in the same culture well. Cell density is even more on polymer regions in comparison to the adjoining glass regions. This hints towards the importance of close proximity polymer surfaces with the neuronal cells. Both of these hypotheses, firstly, whether polymer substrates release any chemical cues to enhance the neuronal cell proliferation and secondly, about further acceleration of proliferation rate need further vigorous investigations. Also, it should be noted that these results are obtained for a neuronal cell line which is a more

### Chapter 3

general set of cells and hence the results should have wider applicability. It opens the possibilities for manipulating the neurons other than the retinal neurons as well. Other aspects apart from the proliferation like differentiation, axonal growth of neurons, formation of functional synapses are the questions yet to be investigated. Also, part of the experiments explained before are under progress.

## CHAPTER 4

# Summary & Future Directions

Advanced materials carry the potential for serving as key to the development and design of new implant technologies. Situations become more challenging when it comes to prosthesis for sensory organs where functional materials with ability to perform sensory tasks are required. Optoelectronic polymers have shown promising possibilities in the recent past in the case of visual prosthesis. However, there are still many open ended questions which are necessary to address before embarking on the clinical implants. Few of such questions like long term functionality and stability of optoelectronic devices in biological environments and biocompatibility of these materials have been addressed in this thesis.

The first part of the thesis focused on the optoelectronic properties of the interface between BHJ system and electrolytes. The photoillumination of BHJ/interface results in interesting photophysical features. It is shown that the photoelectric signals diminish over long durations. This can be a big hurdle in use of these materials in medical implants and needs to be addressed urgently. Possible routes will depend on mechanism of degradation. It is possible to fabricate the devices with deeper LUMO levels. These interfaces have the potential for construction of new devices with equal applications in the biological world. However, a more detailed characterization of these structures is needed. For instance, the exact mechanism for the unique transient behavior in response to light needs further insights. This will enable biomimicking visual process to a higher

## Chapter 4

degree. Also, the transient response is found to be dependent on many parameters like thickness and composition of polymer layer, concentration and nature of electrolyte as well as wavelength and intensity of light. Interfacing these materials with biological system further adds to the complexity as well as to utility. Factors involved in deciding temporal characteristics can be optimized so as to enable targeted firing events in neurons. Patterning of the films or the electrodes can also provide spatial information. It is necessary to understand the behavior of these interfaces governed by aforementioned parameters which is the one of the future direction.

The other part of the thesis deals with the integrity of the biological systems in the presence of optoelectronic polymers in close proximity. As evident from the results, SH-SY5Y cell line shows better growth on polymer surface in comparison to glass surface. These trends of specific type of cells and their affinity towards certain surfaces need to be understood. These results are obtained for a more general set of cells and hence should be applicable to a wider range of cells. It also indicates that optoelectronic polymers have the ability to manipulate the biological systems in positive directions along with the functional aspects. This supports the notion of accelerated repair mechanisms on the sites where implants are done. Other aspects like differentiation of stem cells, controlled axonal growth, tailor made artificial neural network, spatially resolved optical excitation of neural systems and a complete systems for stimulating, recording and manipulating the neuronal network are among the areas that can be explored in the future.

## REFERENCES

1. Humayun, M.S., et al., *Visual perception elicited by electrical stimulation of retina in blind humans*. Archives of Ophthalmology, 1996. **114**(1): p. 40-46.
2. Humayun, M.S., et al., *Visual perception in a blind subject with a chronic microelectronic retinal prosthesis*. Vision Research, 2003. **43**(24): p. 2573-2581.
3. Humayun, M.S., et al., *Pattern electrical stimulation of the human retina*. Vision Research, 1999. **39**(15): p. 2569-2576.
4. Gautam, V., et al., *A Polymer Optoelectronic Interface Provides Visual Cues to a Blind Retina*. Advanced Materials, 2014. **26**(11): p. 1751-1756.
5. Berggren, M. and A. Richter-Dahlfors, *Organic Bioelectronics*. Advanced Materials, 2007. **19**(20): p. 3201-3213.
6. Owens, R.M. and G.G. Malliaras, *Organic Electronics at the Interface with Biology*. MRS Bulletin, 2010. **35**(06): p. 449-456.
7. Krishnamoorthy, K., et al., *Novel label-free DNA sensors based on poly (3, 4-ethylenedioxythiophene)*. Chem. Commun., 2004(7): p. 820-821.
8. Zhu, Z.-T., et al., *A simple poly (3, 4-ethylene dioxythiophene)/poly (styrene sulfonic acid) transistor for glucose sensing at neutral pH*. Chem. Commun., 2004(13): p. 1556-1557.
9. Duncan, R., *The dawning era of polymer therapeutics*. Nat Rev Drug Discov, 2003. **2**(5): p. 347-360.
10. Abidian, M.R., et al., *Interfacing Conducting Polymer Nanotubes with the Central Nervous System: Chronic Neural Recording using Poly(3,4-ethylenedioxythiophene) Nanotubes*. Advanced Materials, 2009. **21**(37): p. 3764-3770.
11. Richardson-Burns, S.M., et al., *Polymerization of the conducting polymer poly(3,4-ethylenedioxythiophene) (PEDOT) around living neural cells*. Biomaterials, 2007. **28**(8): p. 1539-1552.
12. Ghezzi, D., et al., *A polymer optoelectronic interface restores light sensitivity in blind rat retinas*. Nat Photon, 2013. **7**(5): p. 400-406.
13. Heeger, A.J., *Semiconducting and Metallic Polymers: The Fourth Generation of Polymeric Materials (Nobel Lecture)*. Angewandte Chemie International Edition, 2001. **40**(14): p. 2591-2611.

## References

14. Anna, D., C.K. Frederik, and C. Hongzheng, *Organic photovoltaics*. Nanotechnology, 2013. **24**(48): p. 480201.
15. Burroughes, J., et al., *Light-emitting diodes based on conjugated polymers*. nature, 1990. **347**(6293): p. 539-541.
16. Günes, S., H. Neugebauer, and N.S. Sariciftci, *Conjugated Polymer-Based Organic Solar Cells*. Chemical Reviews, 2007. **107**(4): p. 1324-1338.
17. Sirringhaus, H., *Device physics of solution-processed organic field-effect transistors*. Advanced Materials, 2005. **17**(20): p. 2411-2425.
18. Dodabalapur, A., *Organic light emitting diodes*. Solid State Communications, 1997. **102**(2): p. 259-267.
19. Kulkarni, A.P., et al., *Electron transport materials for organic light-emitting diodes*. Chemistry of materials, 2004. **16**(23): p. 4556-4573.
20. Campbell, I., et al., *Direct measurement of conjugated polymer electronic excitation energies using metal/polymer/metal structures*. Physical review letters, 1996. **76**(11): p. 1900.
21. Halls, J., et al., *Efficient photodiodes from interpenetrating polymer networks*. 1995.
22. Yu, G., et al., *Polymer photovoltaic cells: enhanced efficiencies via a network of internal donor-acceptor heterojunctions*. Science-AAAS-Weekly Paper Edition, 1995. **270**(5243): p. 1789-1790.
23. Heeger, A.J., *25th Anniversary article: bulk heterojunction solar cells: understanding the mechanism of operation*. Advanced Materials, 2014. **26**(1): p. 10-28.
24. Koch, N., *Organic electronic devices and their functional interfaces*. ChemPhysChem, 2007. **8**(10): p. 1438-1455.
25. Kandel ER, S.J., Jessell TM *Principles of Neural Science*. 4th edition ed. 2000: McGraw-Hill, New York.
26. Bellani, S., et al., *Reversible P3HT/Oxygen Charge Transfer Complex Identification in Thin Films Exposed to Direct Contact with Water*. Journal of Physical Chemistry C, 2014. **118**(12): p. 6291-6299.
27. Yohannes, T., T. Solomon, and O. Inganäs, *Polymer-electrolyte-based photoelectrochemical solar energy conversion with poly (3-methylthiophene) photoactive electrode*. Synthetic metals, 1996. **82**(3): p. 215-220.



28. Nattestad, A., et al., *Highly efficient photocathodes for dye-sensitized tandem solar cells*. *Nature materials*, 2010. **9**(1): p. 31-35.
29. Xia, Y., et al., *Carrier localization on surfaces of organic semiconductors gated with electrolytes*. *Physical review letters*, 2010. **105**(3): p. 036802.
30. Bressers, P., et al., *Visible light emission from a porous silicon/solution diode*. *Applied physics letters*, 1992. **61**(1): p. 108-110.
31. Arutyunyan, V.M., *Physical properties of the semiconductor-electrolyte interface*. *Soviet Physics Uspekhi*, 1989. **32**(6): p. 521.
32. Tomkiewicz, M., *Impedance spectroscopy of rectifying semiconductor-electrolyte interfaces*. *Electrochimica Acta*, 1990. **35**(10): p. 1631-1635.
33. Tan, M.X., C.N. Kenyon, and N.S. Lewis, *Experimental Measurement of Quasi-Fermi Levels at an Illuminated Semiconductor/Liquid Contact*. *The Journal of Physical Chemistry*, 1994. **98**(19): p. 4959-4962.
34. Kovács, I.K. and G. Horvai, *Possibilities of chemical sensing at the semiconductor/electrolyte interface*. *Sensors and Actuators B: Chemical*, 1994. **19**(1-3): p. 315-320.
35. Memming, R. and G. Schwandt, *Potential distribution and formation of surface states at the silicon-electrolyte interface*. *Surface Science*, 1966. **5**(1): p. 97-110.
36. Gerischer, H., *The impact of semiconductors on the concepts of electrochemistry*. *Electrochimica Acta*, 1990. **35**(11-12): p. 1677-1699.
37. Licht, S., *Multiple Band Gap Semiconductor/Electrolyte Solar Energy Conversion*. *The Journal of Physical Chemistry B*, 2001. **105**(27): p. 6281-6294.
38. Narayan, K.S., et al., *Water-Gated Phospholipid-Monolayer Organic Field Effect Transistor Through Modified Mueller-Montal Method*. *Electron Device Letters, IEEE*, 2013. **34**(2): p. 310-312.
39. Gautam, V., M. Bag, and K.S. Narayan, *Single-Pixel, Single-Layer Polymer Device as a Tricolor Sensor with Signals Mimicking Natural Photoreceptors*. *Journal of the American Chemical Society*, 2011. **133**(44): p. 17942-17949.
40. Srivastava, N., et al., *Neuronal Differentiation of Embryonic Stem Cell Derived Neuronal Progenitors Can Be Regulated by Stretchable Conducting Polymers*. *Tissue Engineering Part A*, 2013. **19**(17-18): p. 1984-1993.
41. Schloesser, M., et al. *Embedded device for simultaneous recording and stimulation for retina implant research*. in *SENSORS, 2013 IEEE*. 2013.

## References

42. Benfenati, V., et al., *A transparent organic transistor structure for bidirectional stimulation and recording of primary neurons*. *Nat Mater*, 2013. **12**(7): p. 672-680.
43. Khodagholy, D., et al., *In vivo recordings of brain activity using organic transistors*. *Nat Commun*, 2013. **4**: p. 1575.
44. Kergoat, L., et al., *Detection of Glutamate and Acetylcholine with Organic Electrochemical Transistors Based on Conducting Polymer/Platinum Nanoparticle Composites*. *Advanced Materials*, 2014. **26**(32): p. 5658-5664.
45. Nagai, N., et al., *A Platform for Controlled Dual-Drug Delivery to the Retina: Protective Effects against Light-Induced Retinal Damage in Rats*. *Advanced Healthcare Materials*, 2014. **3**(10): p. 1555-1560.
46. Richardson, R.T., et al., *Polypyrrole-coated electrodes for the delivery of charge and neurotrophins to cochlear neurons*. *Biomaterials*, 2009. **30**(13): p. 2614-2624.
47. Richardson, R.T., et al., *The effect of polypyrrole with incorporated neurotrophin-3 on the promotion of neurite outgrowth from auditory neurons*. *Biomaterials*, 2007. **28**(3): p. 513-523.
48. Gautam, V., M. Bag, and K.S. Narayan, *Dynamics of Bulk Polymer Heterostructure/Electrolyte Devices*. *The Journal of Physical Chemistry Letters*, 2010. **1**(22): p. 3277-3282.
49. Rivnay, J., et al., *Unconventional Face-On Texture and Exceptional In-Plane Order of a High Mobility n-Type Polymer*. *Advanced Materials*, 2010. **22**(39): p. 4359-4363.
50. Schuettfort, T., et al., *Surface and Bulk Structural Characterization of a High-Mobility Electron-Transporting Polymer*. *Macromolecules*, 2011. **44**(6): p. 1530-1539.
51. Nikkhah, M., et al., *Engineering microscale topographies to control the cell-substrate interface*. *Biomaterials*, 2012. **33**(21): p. 5230-5246.
52. Scarpa, G., et al., *Biocompatibility Studies of Functionalized Regioregular Poly(3-hexylthiophene) Layers for Sensing Applications*. *Macromolecular Bioscience*, 2010. **10**(4): p. 378-383.
53. Ratner, B.D. and S.J. Bryant, *BIOMATERIALS: Where We Have Been and Where We are Going*. *Annual Review of Biomedical Engineering*, 2004. **6**(1): p. 41-75.
54. Adler, R., J. Jerdan, and A.T. Hewitt, *Responses of cultured neural retinal cells to substratum-bound laminin and other extracellular matrix molecules*. *Developmental Biology*, 1985. **112**(1): p. 100-114.

## References

55. Smalheiser, N.R., S.M. Crain, and L.M. Reid, *Laminin as a substrate for retinal axons in vitro*. Developmental Brain Research, 1984. **12**(1): p. 136-140.
56. Scarpa, G., et al. *Biocompatibility studies of solution-processable organic thin-film transistors for sensing applications*. in *Nano/Molecular Medicine and Engineering (NANOMED), 2009 IEEE International Conference on*. 2009.
57. Gattazzo, F., et al., *Realisation and characterization of conductive hollow fibers for neuronal tissue engineering*. Journal of Biomedical Materials Research Part B: Applied Biomaterials, 2014: p. n/a-n/a.



# Appendix

## Arduino Code for Photoillumination Setup

```
Int i;

void setup () {
    // initialize the digital pins as an output.
    for (i=0;i<14;i++){
        pinMode (i, OUTPUT );
    }
}

void loop () {
    // the loop routine runs over and over again forever:
    for (i=0;i<14;i++){
        analogWrite (i, 20);
    }
    // turn the LED on (HIGH is the voltage level)
    delay (1000);
    // wait for a second
    for (i=0;i<14;i++){
        analogWrite (i, LOW);
    }
    // turn the LED off by making the voltage LOW
    delay (1000);
    // wait for a second
}
```

# LabVIEW Program for Interfacing Arduino and Oscilloscope

## Front Panel

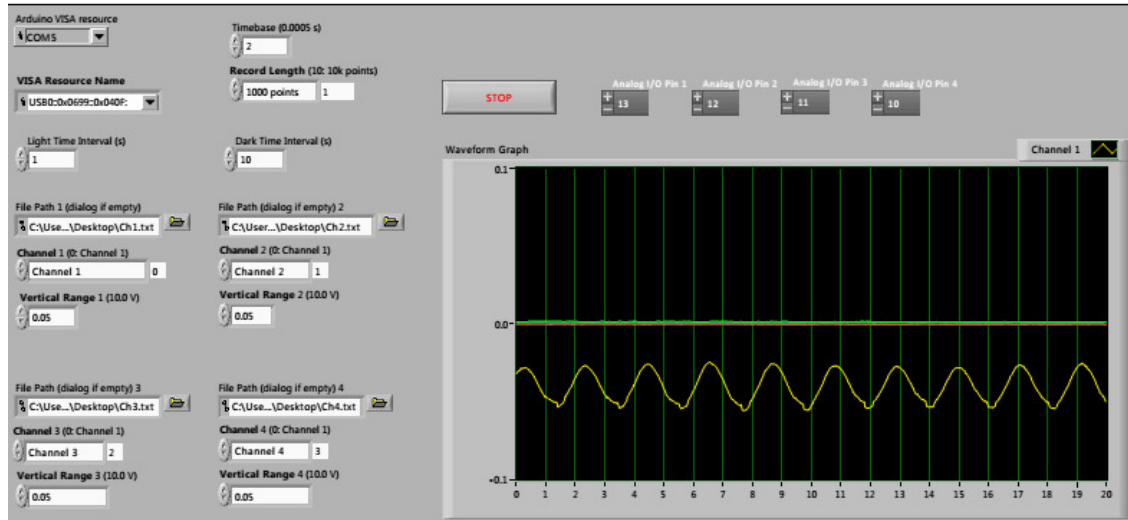


Figure: Front Panel for LabVIEW Program